

CHARACTERIZATION OF THE NASHVILLE URBAN PLUME
ON JULY 3 AND JULY 18, 1995

L. J. Nunnermacker,¹ D. Imre,¹ P.H. Daum,¹ L. Kleinman,¹ Y-N Lee,¹ J. H. Lee,¹ S. R. Springston,¹
L. Newman,¹ J. Weinstein-Lloyd,² W. T. Luke,³ R. Banta,⁴ R. Alvarez,⁴ C. Senff,⁴ S. Sillman,⁵
M. Holdren,⁶ G. W. Keigley,⁶ and X. Zhou⁷

September 1998

Accepted for publication in
Journal of Geophysical Research

¹ Environmental Chemistry Division, Department of Applied Science, Brookhaven National Laboratory, Upton, New York.

² Chemistry/Physics Department, State University of New York, Old Westbury.

³ Air Resources Laboratory, NOAA, Silver Spring, Maryland.

⁴ Environmental Resources Laboratory, NOAA, Boulder, Colorado.

⁵ Department of Atmospheric, Oceanic and Space Sciences, University of Michigan, Ann Arbor.

⁶ Battelle-Columbus, Atmospheric Science and Applied Technology, Columbus, Ohio.

⁷ New York State Department of Health, Albany.

By acceptance of this article, the publisher and/or recipient acknowledges the U.S. Government's right to retain a non exclusive, royalty-free license in and to any copyright covering this paper.

This research was performed under the auspices of the U.S. Department of Energy under Contract No. DE-AC02-98CH10886.

Characterization of the Nashville urban plume on July 3 and July 18, 1995

L. J. Nunnermacker,¹ D. Imre,¹ P.H. Daum,¹ L. Kleinman,¹ Y.-N. Lee,¹ J. H. Lee,¹ S. R. Springston,¹ L. Newman,¹ J. Weinstein-Lloyd,² W. T. Luke,³ R. Banta,⁴ R. Alvarez,⁴ C. Senff,⁴ S. Sillman,⁵ M. Holdren,⁶ G. W. Keigley,⁶ and X. Zhou⁷

Abstract. This paper reports results from the Southern Oxidants Study field campaign designed to characterize the formation and distribution of ozone and related species in the Nashville urban region. Data from several airborne platforms as well as surface observations on July 3 and 18 are examined to gain insight into the factors that control O₃ formation rates and concentrations in the regional plumes. On both days, well-defined urban and power plant plumes were sampled. Utilizing both aircraft and surface data, a detailed kinetic analysis of the chemical evolution of the urban plume is performed to derive NO_x lifetime, ozone production efficiency, OH concentration, HNO₃ dry deposition rate, and the relative importance of natural and anthropogenic hydrocarbons to O₃ production. Analysis of the urban plume data revealed a very active photochemical system (average [OH] ~1.2 x 10⁷ molecules cm⁻³) which consumed 50% of the NO_x within approximately 2 hours, at an ozone production efficiency of 2.5 to 4 molecules for each molecule of NO_x. Anthropogenic hydrocarbons provided approximately 44% of the fuel for ozone production by the urban plume. The dry deposition rate for HNO₃ in the urban plume was estimated to be of the order of 5 to 7 cm s⁻¹.

1. Introduction

Similar to many urban areas in the southeastern United States, Nashville has had difficulty attaining compliance with current National Ambient Air Quality Standards for O₃. Although standard O₃ control strategies have been implemented for some time, O₃ levels in the southeastern United States have not decreased measurably [Chameides *et al.*, 1992; Chameides and Cowling, 1995]. The 1995 Southern Oxidants Study (SOS-Nashville/Mid Tennessee) was part of an effort to unravel the process of ozone production [National Academy of Sciences, 1991] so that different emission control strategies could be investigated [Sillman, 1993].

Nashville is a moderately sized city with a population of 0.5 million people in the downtown and surrounding metropolitan area. It is the only major metropolitan area in central Tennessee and for this reason air quality is not significantly influenced by transport of fresh emissions from other urban areas. However, similar to many other U.S. cities of this size, Nashville is itself a significant source of oxides of nitrogen (NO_x), carbon monoxide (CO), and volatile organic compounds (VOCs) from automotive and industrial sources. The area around Nashville is also the location of several large fossil fuel power plants that emit significant quantities of NO_x. In combination with the meteorology prevailing during the summer season, these emissions cause the formation of a relatively high background concentration of O₃ (50-80 ppbv) and related photochemical product species such as aldehydes, peroxides, and fine aerosols that are present throughout the region at all hours of the day. During the summer, high background O₃ concentrations, high humidity, and intense solar radiation produce a chemical environment in which

fresh emissions of NO_x (catalyst) and hydrocarbons (fuel) react rapidly to form additional ozone. Fresh catalyst emissions from the multitude of power plants give rise to localized plumes characterized by high NO_y (NO_y is defined as the sum of oxides of nitrogen including NO, NO₂, HNO₃, peroxyacetyl nitrate (PAN), alkyl nitrates and aerosol nitrates; see Fehsenfeld *et al.*, [1987] and Williams *et al.*, [1998]) and SO₂ concentrations [Joos *et al.*, 1990; Duncan *et al.*, 1995]. Though slightly more diffuse, the urban plume can be identified and distinguished from the power plants by its characteristic combination of high NO_y and CO concentrations and relatively low SO₂ levels.

Both biogenic and anthropogenic sources contribute fuel for this very active photochemical system [Chameides *et al.*, 1988]. The urban center is a source of anthropogenic hydrocarbons with downtown nonmethane nonisoprene hydrocarbons (NMNIHC, also excluding CO and formaldehyde) concentrations reaching >75 ppb C (parts per billion carbon). High background concentrations of anthropogenic hydrocarbons are present throughout the region and carbon monoxide background concentrations were usually greater than 150 ppbv. Forested areas around Nashville are a significant source of isoprene, the major biogenic hydrocarbon in the region, exhibiting a highly non uniform distribution and concentrations between 0.1 and 10.0 ppb C. Local emission of biogenic hydrocarbons is of particular relevance to Nashville because of the presence of large point sources of NO_x in the area surrounding the city. In this paper the relative contribution of anthropogenic and biogenic hydrocarbons to O₃ production in an urban plume was determined.

This paper presents data obtained on 2 days of measurements, July 3 and July 18, during which the urban plume was sampled

¹Environmental Chemistry Division, Department of Applied Science, Brookhaven National Laboratory, Upton, New York.

²Chemistry/Physics Department, State University of New York, Old Westbury.

³Air Resources Laboratory, NOAA, Silver Spring, Maryland.

⁴Environmental Resources Laboratory, NOAA, Boulder, Colorado.

⁵Department of Atmospheric, Oceanic and Space Sciences, University of Michigan, Ann Arbor.

⁶Battelle-Columbus, Atmospheric Science and Applied Technology, Columbus, Ohio.

⁷New York State Department of Health, Albany.

under similar meteorological conditions (i.e., moderate wind speeds). On July 3 winds were from the southwest and background concentrations of ozone and other photochemical product species were high. Four research aircraft flew on July 3 and were used to characterize the background conditions in the region, as well as the physical distribution and chemical properties of the urban plume. On July 18, we will be mainly describing measurements taken on the DOE G-1. Winds were from the northeast and background concentrations of ozone, ozone precursors, and photochemical products were among the lowest observed during the entire program.

In the first half of this paper we provide a descriptive picture of the Nashville area chemical environment. In the second half we examine the data and perform a semi-quantitative analysis of chemical processes that occurred in the Nashville plume as it advected downwind and chemically transformed.

2. Instrumentation

2.1. DOE G-1

Oxides of nitrogen (NO , NO_x , and NO_y) were measured using a three channel [Williams *et al.*, 1998; Daum *et al.*, 1996; Kleinman *et al.*, 1994] NO/O_3 chemiluminescence instrument; NO was measured directly, NO_2 by conversion with UV-photolysis, and NO_y by reduction on a hot (350°C) Mo catalyst. Enhancements for the SOS program included use of a Sorbios O_3 generator to provide $[\text{O}_3]$ at 6-7% and addition of H_2O to the O_3 gas stream to maintain constant humidity and reduce background luminescence in the reaction chamber. Sample air for the instrument was provided by a ram air inlet consisting of ~ 0.5 m of 1.3 cm OD perfluoroalkoxy (PFA) Teflon tubing vented at the back of the instrument. The residence time in this inlet was measured to be 15 ms. Instrument response was determined by multipoint calibrations on the ground, and in-flight standard additions of approximately 10 ppbv of NO . The efficiencies of the photolytic and molybdenum converters were $26.9 \pm 0.7\%$ and $97.5 \pm 2\%$, respectively, as determined by gas phase titration of NO with O_3 . Based upon variations of in-flight instrument zeroes and standard additions, the uncertainty in measurement of the NO concentration for 10 s averaged data is estimated to be 20 parts per trillion by volume (pptv) + 15% of the NO concentration, 20 pptv + 15% of the NO_2 concentration, and 50 pptv + 15% of the NO_y concentration.

Ozone was measured using a commercial UV absorption detector (Thermo Environmental Instruments, Model 49-100). The O_3 detector was calibrated before and after the field program; periodic in-flight zeroes were obtained using a charcoal trap. The estimated uncertainty in the O_3 concentration is 5%. Sulfur dioxide measurements were made using a pulsed fluorescence detector (Thermo Environmental Systems, Model 43S) that had been modified to decrease response time to less than 30 s (D. D. Parrish, private communication, 1994). In-flight zeroes were obtained by periodically switching sample air through a carbonate impregnated filter [Leahy *et al.*, 1995]. Instrument response was determined using multipoint calibrations on the ground and standard additions of ~ 20 ppbv SO_2 in flight. Uncertainty in the SO_2 measurement was on the order of 200 pptv + 15% of the ambient concentration for 30 s averaged data. Carbon monoxide was measured using a nondispersive infrared detector (Thermal Environmental Systems, Model 48)

modified according to the design of Dickerson and Delany [1988]. In addition, the White cell was pressurized to 1.25 atm to improve sensitivity and to eliminate the necessity for pressure corrections with altitude. A National Institute of Standards and Technology (NIST) referenced CO standard was used to perform multipoint calibrations on the ground. During flight, zeroes were performed automatically every 10 min by passing ambient air through a hopcalite trap to remove the CO . Instrument uncertainty for 1 min averaged data is estimated to be 30 ppbv + 15% of the measured concentration.

Peroxides were measured with a three-channel continuous flow analyzer using a different chemistry in each channel to speciate H_2O_2 , methylhydroperoxide (MHP), and hydroxymethyl hydroperoxide (HMHP) [Lee *et al.*, 1990; Lee *et al.*, 1993; Lee *et al.*, 1994]. Details of the operation of this instrument during the SOS program are given in a companion paper [Weinstein-Lloyd *et al.*, 1998].

Formaldehyde, glycol aldehyde, glyoxal, methyl glyoxal, glyoxylic acid, and pyruvic acid were determined by a liquid scrubbing technique [Lee and Zhou, 1993] that had been modified for use on aircraft [Lee *et al.*, 1996]. Details of the operation of this instrument during the program are given by Lee *et al.* [1998].

Hydrocarbon measurements were made by collecting air samples in electro-polished stainless steel canisters for subsequent analysis at York University (North York, Ontario, Canada) [Keiser and Young, 1996]. Samples were analyzed by cryogenic preconcentration followed by separation and quantitation with a gas chromatograph employing a flame ionization detector. The uncertainty in the hydrocarbon measurements is typically $\pm 10\%$ or 5 pptv, whichever is larger.

Peroxyacetyl nitrate (PAN) was measured by capillary gas chromatography (Shimadzu GC-Mini 2) equipped with an electron capture detector, a gas sampling valve, and a stainless steel sample loop for direct analysis of air every 8-9 min. The minimum PAN mixing ratio that could be measured by this instrument was approximately 70 pptv. Multipoint PAN calibrations were performed using the procedures reported by Holdren and Spicer [1984].

2.2. Other Instrumentation

Instrumentation packages for the NOAA-AL WP-3D Orion, the NOAA-ETL CASA 212, and the NOAA-ARL Twin Otter are described by Hübler *et al.* [1998]. Surface measurements of NO , NO_y , O_3 , CO and hydrocarbons were made in the center of downtown Nashville, at the corner of 5th and Deadrick Avenues (36.16° latitude and -86.78° longitude), at the top of the James K. Polk Office Building [Kleinman *et al.*, 1998]. This site was operated by Tennessee Valley Authority (TVA) [Meagher *et al.*, 1996], and hydrocarbon samples were collected and analyzed by the University of Miami [Apel *et al.*, 1995].

3. Observations

3.1. July 3, 1995

3.1.1. Meteorology. Synoptic conditions on July 3 were dominated by a high-pressure system located to the north of Nashville. In the early morning ($\sim 06:00$; all times reported as local standard time), the winds had shifted from the northeast to

the southwest at 3–4 m s⁻¹. These southwesterly winds transported the Nashville urban plume to the northeast of the urban area.

Boundary layer heights as measured during the G-1 soundings upwind and downwind of Nashville were 1000 and 1600 m, respectively. Mixing layer height was also obtained from the National Oceanic and Atmospheric Administration (NOAA) radar profilers deployed at Hendersonville, Youth Inc., and Dickson SOS sites. The 12:30 boundary layer height at the Dickson site (50 km to the northwest of Nashville), was 1060 m and at the Hendersonville and Youth Inc. sites (close to downtown Nashville), was 1600 m. The reason for the upwind-downwind difference in these heights is not known but may arise from the heat island effect of the urban area. This effect has been previously observed [Trainer *et al.*, 1995; Hildebrand and Ackerman, 1984; Spangler and Dirks, 1974].

3.1.2. Flight tracks. On July 3, four aircraft flights were made to characterize the Nashville urban plume and the surrounding area. The DOE G-1 departed at approximately noon and flew for about 4 hours (Plate 1). An upwind transect was flown southwest of the city to characterize background composition, then two transects were flown approximately 50 and 80 km northeast of the city (DW1 and DW2). Each transect was flown at altitudes of 600, 1200, and 1800 m. As shown in Plate 1, the Nashville urban plume was encountered during the latter set of transects northeast of the city. Wind speeds from the profiler network indicated that by the first downwind transect (DW1) the urban plume was approximately 5 hours downwind of the city center, and by the second transect (DW2) it was about 7 hours downwind.

The NOAA-AL WP-3D Orion left Nashville at 06:00 and flew east-west transects to the southeast and north of the city and flew north-south transects to the east of the city, Figure 1a. The NOAA-ARL Twin Otter flew between two fixed points downwind of Nashville from 10:40 to 15:11 at several different altitudes (500, 825, and 1250 m) Figure 1b. For purposes of this study only the 500 m transect was examined. The NOAA-ETL CASA 212 departed from Nashville in the late morning and flew two upwind transects and three downwind transects at an almost constant altitude of 2700 m (Figure 1c).

3.1.3. Urban center measurements. Measurements of CO, NO_y, and O₃ at the downtown station are shown in Figures 2a and 2b. Unusually high concentrations of CO (1500 ppbv) and NO_y (130 ppbv) were observed from early to mid morning, 06:00 to 10:00. At the same time, ozone concentrations dropped to almost zero, due to titration of the O₃ by freshly emitted NO. The unusually high concentrations of pollutants in the downtown area during the morning hours were apparently caused by the low wind speeds in combination with a low nocturnal boundary layer height (~200 m). For these reasons pollutants generated in the downtown area were not mixed vertically, nor advected away from the area. Between 10:30 to 11:00, the wind speed increased, shifted to the southwest, and the nocturnal boundary layer broke up. The concentrations of CO and NO_y dropped quickly to 400 and 15 ppbv, respectively, and the ozone concentration rose to 80 ppbv. The concentration of NMNIHC during the rush hour (07:00) sample was 240 ppb C; the ratio of [NMNIHC]/[CO] was ~0.2. Isoprene concentrations were below the detection limit.

3.1.4. Background measurements. During the early morning flight of the NOAA-WP-3D, to the south and southwest

of the city, [O₃] ranged between 55 and 78 ppbv; CO concentrations were between 270 and 310 ppbv. These measurements are summarized in Table 1. The relatively high early morning O₃ concentrations most likely reflect the residual O₃ from processing of the previous day's emissions in the region.

The NOAA CASA 212 flew upwind of Nashville between 10:25 and 10:55, and measured boundary layer O₃ concentrations of the order of 60 to 80 ppbv (Plate 2) outside of the urban area.

The DOE G-1 made a set of multiple altitude transects (600, 1200, and 1800 m) south of Nashville between 12:00 and 13:30 (Plate 1). A summary of the data collected on this flight is given in Table 2. Concentrations measured during the two transects below the boundary layer (600 and 1200 m) were similar; above the boundary layer (1800 m transect) much lower concentrations were detected. The relatively low NO_x to NO_y ratio (0.1) suggested that the boundary layer air was photochemically well aged. The one PAN sample collected exhibited a concentration of 1.2 ppbv.

A summary of the hydrocarbon data from the G-1 flight is given in Table 3. For the upwind transect, the average concentration of anthropogenic hydrocarbons (NMNIHC) was 12.2 ± 0.7 ppb C. Background isoprene concentrations were highly variable. Accordingly, we choose to segregate the data into regimes of high and low isoprene concentrations (to be discussed in greater detail in the analysis section). The maximum isoprene concentration of 8.54 ppb C was measured to the southwest of Nashville. This area has been identified as a strong source region for isoprene [Goldan *et al.*, 1996]. The average formaldehyde concentration observed during the upwind transect was 3.0 ± 0.9 ppbv.

The average upwind total peroxide concentration was 5.3 ± 0.2 ppbv. The organic peroxide fraction was over 50% ([MHP] = 1.53 ± 0.1 ppbv and [HMHP] = 1.24 ± 0.1 ppbv); the H₂O₂ concentration was 2.54 ppbv.

3.1.5. Urban plume measurements. The DOE G-1 sampled the urban plume at distances of 50 and 80 km to the northeast of Nashville (labeled DW1 and DW2 in Plate 1) in the early afternoon. The trace gas data for the 640 m altitude transect 80 km NE of Nashville is plotted as a function of longitude in Figure 3. The data clearly indicate the presence of two well-defined plumes (see the NO_y and SO₂ traces). The eastern plume (-86.2° longitude) may be identified as coming from the Gallatin power plant as indicated by the high SO₂ and relatively low CO concentrations. The western plume (-86.4° longitude) originated from the urban center, as indicated by the elevated concentrations of O₃, CO, NO_y, and NO_x and relatively low concentrations of SO₂.

The maximum ozone concentration observed in the Nashville plume during both sets of downwind transects was ~115 ppbv. No significant difference in CO concentration (above background) was observed in the plume between the first and second downwind transects (at 1200 m, Table 4) indicating that the plume did not undergo significant dilution between the two transects. Moreover, little difference was observed between the concentrations of O₃ and NO_x (Table 4); for both sets of transects, NO_x was less than 20% of the total NO_y at the center of the plume indicating that ozone production was largely completed. Thus approximately 30–35 ppbv of additional ozone had been produced in the urban plume between the time the air parcel left the Nashville city center (Table 4) and the time it was

sampled ~5 hours later. An additional 2 hours of processing (DW2) did not add significantly to the O_3 concentration.

The average concentrations of anthropogenic hydrocarbons (NMNIHC and CO), and biogenic hydrocarbons (isoprene and formaldehyde (HCHO)) measured in the boundary layer during the two sets of downwind transects are given in Table 3. On average, the NMNIHC were 22 ± 6 ppb C. In general, concentrations of isoprene were less than or equal to 1.0 ppb C for all downwind samples. Average formaldehyde concentrations were approximately 4 ppbv. The average concentration of total peroxide was 5.2 ± 0.4 ppbv and consisted of 2.3 ± 0.2 ppbv H_2O_2 , 1.9 ± 0.3 ppbv MHP, and 1.0 ± 0.1 ppbv HMHP. PAN concentrations in the urban plume ranged from 1.1 to 2.4 ppbv, with an average value of 1.6 ± 0.5 ppbv.

The urban plume was observed by the NOAA-ETL CASA 212 on its return to the airport as it flew northeast of Nashville in the early afternoon. Ozone concentrations measured in the center of the plume were 100 to 120 ppbv at an altitude of 900 m (Plate 2). The NOAA Twin Otter flew northeast of Nashville during the early afternoon at about the same time as the DOE G-1. A plot of the Twin Otter observations, Figure 4, exhibits elevated O_3 , NO_y , and CO concentrations that are consistent with the presence of the urban plume northeast of Nashville.

3.2. July 18, 1995

3.2.1. Meteorology. An east-west oriented cold front moved through Tennessee during the early morning hours bringing cool dry air into the region. The 12 Z Nashville sounding and local wind profilers showed moderate flows from the north and northeast. Wind speeds ranged between 4 and 6 $m\ s^{-1}$ below 1000 m. These winds transported the Nashville urban plume southwest of the city (Plate 3). The atmospheric sounding from the DOE G-1 at approximately 10:00 showed a temperature inversion at circa 1000 m indicating the top of the boundary layer. Below the 1000 m, winds were moderate from the northeast. Boundary layer heights at 12:30 were ~1000 m at the Dickson site and ~1500 m at the Hendersonville and Youth Inc sites. The height of the boundary layer obtained from the Dickson profiler agreed well with the DOE G-1 measurement.

3.2.2. Flight track. The DOE G-1 was the only aircraft flying in the vicinity of Nashville on July 18. The flight track, Plate 3, consisted of a vertical profile about 40 m west of Nashville, east-west transects about 40 km north (upwind), and at 25 (EW1) and 90 km (EW2) south (downwind) of the Nashville urban center, at 10:00 to 14:00 local time. As indicated in Plate 3, both the urban plume and the Gallatin power plant plumes were encountered south of Nashville during EW1. Since the winds advected these plumes in a southwesterly direction, the second downwind transect (EW2) missed the urban plume entirely. However, the single north-south (NS) transect connecting EW1 and EW2 did intersect the urban plume. Based on wind profiler data it is estimated that the urban plume was approximately 2 hours downwind of the city center during EW1, and 3.5 hours downwind of the city during the NS transect.

3.2.3. Urban center measurements. The O_3 , CO, and NO_y concentrations measured at the downtown Nashville surface monitoring station are shown in Figure 5. Pollutant concentrations were modest overnight with 150 and 200 ppbv of CO, 20–40 ppbv of O_3 , and 10–20 ppbv of NO_y observed from midnight to approximately 05:00. After 05:00 pollutant levels rose due to

the early morning rush hour and by 07:30, CO and NO_y concentrations peaked at 550 and 50 ppbv, respectively; O_3 concentrations dropped to between 10 and 15 ppbv because of titration by freshly emitted NO. After 08:00, NO_y and CO concentrations dropped, and by noon they had returned to concentrations roughly the same as the overnight concentrations. In contrast, the O_3 concentration rose after 08:00 and peaked at approximately 90 ppbv in the late afternoon. The 07:00 hydrocarbon sample contained 75 ppb C of NMNIHC; [NMNIHC]/[CO] ratio was ~0.2. The isoprene concentration was 1.44 ppb C (Table 5).

3.2.4. Background measurements. Upwind transects were made in the boundary layer at altitudes of 300, 500, and 630 m, about 40 km north of the city (Plate 3). For the most part, concentrations of O_3 , NO_y , and SO_2 , at all three altitudes, were relatively uniform both vertically and horizontally. The CO concentration was fairly constant at 140 ± 20 ppbv throughout the entire transect. PAN concentrations ranged between 0.6 and 0.8 ppbv. The average background concentrations are listed in Table 6.

Hydrocarbon concentrations measured during the upwind transects were characteristic of a boundary layer that had been modestly influenced by anthropogenic emissions: [NMNIHC] = 20.6 ± 11 ppb C, isoprene = 1.0 ppb C (Table 5). The low isoprene concentrations are typical of the region north of the city. Formaldehyde concentrations were unavailable for this flight. The average background total peroxide concentration was 1.74 ± 0.01 ppbv; the organic peroxide fraction of the total was over 47% ([MHP] = 0.43 ± 0.01 ppbv and [HMHP] = 0.38 ± 0.02 ppbv); the H_2O_2 concentration was 0.93 ppbv.

3.2.5. Urban plume measurements. Measurements were made at three different altitudes 25 km south of the urban center (EW1). Figure 6 shows the longitudinal variation in the trace gas concentrations during the 600 m transect. The O_3 concentration, Figure 6a, exhibited a broad maximum of about 75 ppbv representing about a 14 ppbv increase over background. This O_3 plume was associated with a CO plume, Figure 6b, that exhibited a maximum concentration of ~280 ppbv. The NO_y and NO_x plots, Figures 6c and 6d exhibited two peaks. The western peak (-86.78° longitude) was correlated with CO, indicating an urban source. The eastern NO_x and NO_y peaks (-86.57° longitude) were not associated with a CO peak but were strongly associated with a peak in the SO_2 concentration, Figure 6d, suggesting a power plant source. Wind direction data obtained from the profiler network allowed assignment of the western plume to Nashville, and the eastern plume to the Gallatin power plant. The average hydrocarbon concentrations measured during EW1 are listed in Table 5. The average [NMNIHC] was 15.0 ± 3.6 ppb C, with a maximum of 20 ppb C observed at the center of the plume. The isoprene concentration was 0.68 ± 0.3 ppb C. For EW1 the total peroxide concentration was 1.88 ± 0.17 ppbv, [MHP] = 0.52 ± 0.03 ppbv, [HMHP] = 0.37 ± 0.06 ppbv, and 0.99 ± 0.11 ppbv for H_2O_2 . PAN concentrations measured during EW1 were 0.8 and 1.26 ppbv.

Some important features of the data are apparent in Figure 6. Although the NO_x/NO_y ratio is about the same for the urban and power plant plumes (i.e., ~40%), this indicates that both plumes should be actively producing O_3 . The urban plume exhibits excess O_3 relative to background, whereas the power plant plume exhibits an effect on the O_3 concentration lower than background (see the dip in [O_3] at -86.57° longitude). Despite the fact that the power plant emissions have been processed for

about twice as long as the urban emissions, no excess O_3 was formed. We also note that the ozone plume for Nashville is much broader than the plumes for NO_y , NO_x , and CO, suggesting a difference of the rate of ozone formation at the plume center relative to the edges. A more detailed discussion of the significance of these features is given in the analysis section below.

The urban plume was traversed for a second time at a single altitude (630 m) during the NS transect as indicated in Plate 3. Wind speed data from the profiler network indicate that this plume was 3.5 hours downwind of Nashville by the time it was sampled. Trace gas concentrations for this transect are shown in Figure 7. To clearly show the urban plume, background concentrations have been subtracted. Note that the excess O_3 concentration in the plume (12 ppbv) is nearly the same as observed during EW1 but that the excess CO concentrations are much lower. The latter suggests that the urban plume had been diluted in transit between the two sampling locations. A dilution factor of 1.7 (Table 7) can be derived from the peak CO concentrations measured during EW1 and NS and can be used to infer that approximately 6–7 ppbv of additional O_3 had been formed between these two sampling locations. This O_3 production is consistent with the observed change in the fraction of NO_y present as NO_x from ~60% to ~30% (Figure 7c and d).

The average total peroxide concentration during this transect was 2.47 ± 0.18 ppbv; MHP and HMHP were 0.78 ± 0.05 and 0.53 ± 0.06 ppbv, respectively; H_2O_2 was 1.17 ± 0.18 ppbv. The one PAN sample collected during this transect exhibited a concentration of 1.56 ppbv. No hydrocarbon measurements were made.

4. Analysis

4.1. Urban Plume

The following analysis of ozone production in the urban plume is based on the chemistry and meteorology presented in the previous section. The analysis presented here combines the observational data collected on July 3 and 18 and treats the data as if they were all collected within the same plume at different times (where time is measured as the distance from the urban center to the point of sampling divided by the wind speed). Dilution was calculated using CO as a conservative tracer. This approach assumes that the chemistry on these 2 days is similar. Table 8 presents elapsed times for the Nashville urban samples from the point of emission to the point of sampling. The weighted average of the wind speeds observed at the three wind profiler stations is used to calculate the elapsed times. Based on the standard deviation of this average, we estimate that the uncertainty in the elapsed times is of the order of 30%.

4.1.1. NO_y loss from the plume. Since NO_y and CO are emitted from the same source and CO is a conserved quantity, the rate at which NO_y is lost from the plume can be determined by examining the ratio of NO_y to CO as a function of processing time. Shown in Figure 8 is a plot of CO versus NO_y for downtown Nashville and for the urban plume at different processing times. The CO/ NO_y ratio for the source emissions may be estimated as 10 from the slope of the regression line of the downtown data. This ratio is consistent for the entire SOS downtown data set [Kleinman *et al.*, 1998], and with previous studies [Parrish *et al.*, 1991]. Using this ratio as a starting point,

we examine the data obtained during the downwind transects of the urban plume to determine how the ratio changes as a function of processing time. The CO/ NO_y ratios for three of the urban plume transects are shown in Figure 8. Note that a significant increase in the CO/ NO_y ratio is observed as plume age increased from 2 to 7 hours. We ascribe this increase to the removal of NO_y by dry deposition of HNO_3 . The slopes from the three lower panels in Figure 8 are used to derive a “correcting function” of the observed NO_y concentrations for the effects of dry deposition (i.e., to calculate $[NO_y]_0$).

The ratios of observed $[NO_y]$ to calculated $[NO_y]_0$ are plotted as a function of the processing time in Figure 9 (a point from the NS transect not shown in Figure 8 is also included). As shown in Figure 9, the data combine to yield a simple decay curve for NO_y . The shape of the dotted curve may be explained as follows: The NO_y loss rate is determined by two processes; conversion of NO_x to NO_z and dry deposition of HNO_3 . This type of consecutive kinetics has the same qualitative time dependence as depicted by the dotted line in Figure 9. During the initial stages of plume aging, $[NO_y]/[NO_y]_0$ remains relatively constant because most of the NO_y is present as NO_x . When a larger fraction of NO_x has been converted, the NO_y loss rate increases. The final point in Figure 9 is based on an assumed constant NO_y background of 20%. This fraction may represent PAN and/or the 10–15% NO_x found in aged background air. Although the removal of NO_y from the urban plume is non-exponential, a phenomenological loss rate from the system can be determined by using a $1/e$ lifetime as a guide (i.e. ~37% of the NO_y above background). A phenomenological loss rate for NO_y of 6 hours was estimated from the data shown in Figure 9. With knowledge of the NO_y lifetime, we can now determine the dry deposition rate of HNO_3 .

4.1.2. HNO_3 dry deposition rate. We deduce the HNO_3 dry deposition rate on the assumption that the observed NO_y loss rate reflects only this quantity. We estimate an average boundary layer height of 1200 m to represent the fact that the boundary layer height varied during the observational period between 600 and 1600 m. Using the equation $V_d = H/t$ (H = height of the boundary layer, and t = lifetime of NO_y), we calculate a dry deposition rate of 5.6 ± 1 cm s^{-1} for HNO_3 . This deposition rate is similar to estimates made by Huebert and Robert [1985] and is supported by recent measurements of by Hall and Claiborne [1997] who reported a dry deposition for rate H_2O_2 of 6 cm s^{-1} . Agreement between HNO_3 and H_2O_2 dry deposition rates can be expected if both species deposit at the aerodynamic limit [Watkins *et al.*, 1995].

4.1.3. Ozone production efficiency. Ozone production efficiency with respect to NO_x (OPEx) is a central quantity in emission control strategies since it is a measure of how many O_3 molecules are produced by each NO_x before it is lost from the catalytic cycle [Trainer *et al.*, 1995]. For a plume it may be defined as

$$OPEx = [(O_3 + NO_2)]/[cNO_x] \quad (1)$$

where $(O_3 + NO_2)$ is the concentration of odd oxygen, denoted oddO, and $[(O_3 + NO_2)]$ is the difference between the odd oxygen in the plume and the background; $[cNO_x]$ is the amount of NO_x that was consumed and is defined as $[cNO_x] = ([NO_y]_0 - [NO_x])$; $[NO_y]_0$ is $[NO_y]$ corrected for depositional losses and is therefore a measure of how much NO_x was actually emitted. OPEx has customarily been estimated from the relationship

between O_3 and NO_x , implicitly assuming that NO_y is a conserved quantity and therefore that $NO_z = cNO_x$. Although it has been recognized that O_3 production efficiency derived in this way may be over estimated [Trainer *et al.*, 1993], the effect has for the most part been neglected. Below we present a simple method for estimating the NO_z loss rate and determining the true O_3 production efficiency using CO as an inert tracer. After correcting NO_y concentrations for losses due to dry deposition of HNO_3 , ozone production efficiencies for the Nashville urban plume were determined. OPEX was calculated using cross-plume integrals of O_3 and cNO_x (Figure 3; i.e., the above-background area under the curve for the urban plume). For the four transects of the urban plume that were made on July 3 at 500 and 1200 m on DW1 and DW2 an average OPEX of 3.2 ± 0.9 was calculated. The data obtained on July 18 during EW1 yielded an average OPEX of 3.4 ± 1 . These calculated OPEX values are in excellent agreement with Sillman *et al.* [1998]; however, they are significantly lower than OPEX values reported for other urban plumes [e.g., Trainer *et al.*, 1995; Olszyna *et al.*, 1994], possibly because these previous estimates did not adequately account for losses by dry deposition of HNO_3 .

The above procedure, while providing an accurate estimate of the average OPEX does not address the issue of variations in O_3 production efficiency across the plume (i.e., from plume center to plume edge). In Figures 10a and 10b, we present a study of the variation of OPEX across the urban plume. As pointed out above, OPEX has customarily been determined from the slope of a linear fit to plots of O_3 versus NO_z [Trainer *et al.*, 1995; Olszyna *et al.*, 1994]; implicit in this procedure are the assumptions that a linear function is a reasonable representation of the O_3 to NO_z relationship and that prior to the measurements no NO_z was lost. In order to avoid the need for these assumptions we account for dry deposition by replacing NO_z with a true value of consumed NO_x (cNO_x) which we determine on the basis of the difference $[NO_y]_0 - [NO_x]$. Second, we do not assume a linear relation between O_3 and cNO_x but instead examine the non linearity to obtain more detailed information. Figure 10 shows plots of $[O_3+NO_2]$ and derived OPEX versus cNO_x for the combined DW1 and DW2 on July 3 (Figure 10a) and EW1 on July 18 (Figure 10b) (including urban plume data only).

The data from July 3 (Figure 10a) shows a slight curvature in the $[O_3+NO_2]$ versus cNO_x function indicative of slightly lower OPEX at the plume center. The smooth curve through these data is a quadratic least squares fit, $F(cNO_x)$; $[O_3+NO_2] = F(cNO_x)$. We use this function as the basis to calculate the dependence of OPEX on cNO_x according to the following:

$$OPEX = [F(cNO_x)]/[cNO_x] \quad (2)$$

where $[]$ indicates quantity above background. The calculated OPEX shown in Figure 10a demonstrates that on July 3 the efficiency only ranged from 2.6 at the plume center to 4.5 at the plume edges. The apparent rapid rise in OPEX at low cNO_x is an artifact of division of two small numbers at low cNO_x .

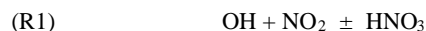
The equivalent $[O_3+NO_2]$ versus cNO_x plot for the July 18 data shown in Figure 10b shows a more pronounced non-linearity consistent with the plume's younger chemical age. This becomes more evident in the plot of calculated OPEX versus cNO_x which shows that the O_3 production efficiency increases by over a factor of 2 from plume center to plume edge. Consistent with the slightly lower NO_x levels on that day, we

note that the overall OPEX on July 18 was somewhat higher than that observed on July 3.

On the basis of the two modes of analysis, we report a range of OPEX from 2.3 to 4.4 for the Nashville urban plume on these mildly polluted days. These values are in agreement with ozone production efficiencies determined by Daum *et al.* [1996], when the sampled air was isolated from depositional losses.

4.1.4. NO_x lifetime. As the catalyst for O_3 production, it is important to determine the rate at which NO_x is lost from the catalytic cycle producing O_3 via conversion to the photochemically unreactive NO_z . This removal rate is not straightforward to derive from changes in the $[NO_x]/[NO_y]$ ratio since this ratio is also influenced by depositional losses of HNO_3 from the system. However, we can compensate for the loss of NO_y by using the dry deposition rate for HNO_3 derived above, in combination with the age of the plume to calculate $[NO_y]_0$. The ratio $[NO_x]/[NO_y]_0$ is a measure of the fraction of NO_x lost to the photochemistry mostly by conversion to HNO_3 . In Figure 11, we present a study of the evolution of this ratio for the four transects. Figure 12 is a summary of these data in a plot of $[NO_x]/[NO_y]_0$ versus time (plume age) for the transects of the Nashville plume (Table 8). We have assumed for this plot that $[NO_x]_0 = [NO_y]_0$ at point of emission. The data fit an exponential decay, with a $1/e$ lifetime of 2.1 ± 0.7 hours, indicative of an extremely rapid photochemistry.

4.1.5. OH concentrations. The dominant process for NO_x removal is the reaction



Since the rate constant for this reaction is known ($1.1 \times 10^{-11} \text{ cm}^3 \text{ molecule}^{-1} \text{ s}^{-1}$ at 298°K, 1 atm [Finlayson-Pitts and Pitts, 1986], we can use our calculated removal rate of NO_x to determine the average OH concentration by using the following formula: $NO_2 = (k*[OH])^{-1}$. Using the NO_x lifetime (in the urban plume) of 2.1 hours, we estimate an OH concentration of $1.2 \pm 0.4 \times 10^7 \text{ molecules cm}^{-3}$. Results from the model for Nashville described by Sillman *et al.* [1998] show OH concentrations at noon in the Nashville urban plume equal to $1.2 - 1.4 \times 10^7 \text{ molecules cm}^{-3}$, consistent with this estimate.

4.1.6. Hydrocarbons. Presented here is an analysis of the hydrocarbon data obtained during the July 3 and 18 flights. Hydrocarbon samples were collected at relatively sparse intervals, therefore this analysis follows a slightly different approach from the one used above. The average $[NMNIHC]/[CO]$ ratio in the downtown data for July 3 and 18 was $0.25 \pm 0.4 \text{ ppb C/ppbv}$. Since the more reactive of these hydrocarbons were rapidly consumed, this ratio dropped quickly as the plume advected away from the urban center and the $[NMNIHC]/[CO]$ ratio of the plume hydrocarbon samples soon became indistinguishable from the background samples. For this reason, as well as the sparseness of the data, it was often difficult to detect a clear urban plume signature for NMNIHC. An exception was the EW1 transect on July 18, when the urban plume was sampled close to the source region. Figure 13 shows the NMNIHC concentrations from EW1 at all three altitudes superimposed on a plot of the composite CO concentration for these three transects. This plot clearly shows the presence of a NMNIHC signature in the urban plume. Figure 14 shows the same data in a plot of the NMNIHC versus CO, where the $[CO]$ is the average CO concentration measured during collection of each hydrocarbon sample. The CO and NMNIHC

concentrations are highly correlated with a slope of 0.11 which is more than a factor of 2 lower than the downtown ratio of 0.25 ± 0.4 indicating that more than 50% of the anthropogenic hydrocarbons had been oxidized in the first 2 hours of plume evolution.

The NMNIHC in the Nashville source region consists of a mixture of hydrocarbons with a wide range of reactivities. This results in large differences in the extent to which various hydrocarbons are consumed as the urban plume advects downwind and reacts. If reaction with OH is the principal sink for these hydrocarbons, their concentration should obey a first-order rate law: $[\text{NMNIHC}]/[\text{NMNIHC}]_0 = e^{(-k't)}$ (where $k' = k_{\text{OH}}[\text{OH}]$ and k_{OH} is the individual rate constant for reaction of OH with each hydrocarbon). Figure 15 is a plot of the fraction of unreacted NMNIHC between the downtown and the EW1 transect for each of the sampled hydrocarbons (i.e., the left-hand side of the above equation) versus k_{OH} , after correcting the $[\text{NMNIHC}]$ for dilution by normalizing to the CO concentration. The solid line in Figure 15 is an exponential fit of the data to k_{OH} , yielding an $[\text{OH}] = 1.15 \times 10^7 \text{ molecules cm}^{-3}$, in excellent agreement with our estimate of the OH concentration calculated from the NO_2 oxidation rate (see solid black square in Figure 15).

Below we attempt to assess the relative contribution of biogenic versus anthropogenic hydrocarbons to ozone production in the urban plume. First, we examine the distribution of the observed isoprene concentrations for the two flights. Isoprene varied from below the detection limit ($<100 \text{ pptv}$) to 10 ppb C , from one location to the next, consistent with the localized nature of isoprene sources. Figure 16 illustrates the distribution of observed isoprene concentrations during the entire SOS field campaign. We have somewhat arbitrarily segregated the data into high and low isoprene regimes at 2 ppb C . Most of the samples clearly belong in the low concentration regime. The urban plume isoprene data, for July 3 and 18, are consistent with the low isoprene regime.

For this reason, the approximate source apportionment between anthropogenic and biogenic hydrocarbons is calculated on the basis of hydrocarbon reactivity under low isoprene conditions for the urban plume. The hydrocarbon reactivity is defined as the hydrocarbon concentration (i.e., NMNIHC, CO, isoprene + methacrolein (MAC) + methyl vinyl ketone (MVK), formaldehyde (HCHO), or methane (CH_4) multiplied by its reactivity to OH and the number of carbons contributing to O_3 production. This value is then divided by the total reactivity to obtain the percent contribution of each hydrocarbon. The concentrations and reactivities of the secondary products from O_3 formation that could continue to participate in the chemistry were not determined. Therefore the analysis described here must be considered approximate.

The hydrocarbon apportionment for ozone formation in the urban plume within the first 2 hours of its evolution is shown in the first column of Table 9. Over this relatively short time period, ozone production is dominated by the more reactive anthropogenic hydrocarbons. It is important to note that despite their low concentrations, biogenic hydrocarbons (taken here to include contributions from isoprene, MVK, MAC, and HCHO) contribute approximately 25% of the fuel to the O_3 production in the urban plume at the early stages of the plume's evolution. The role of biogenic hydrocarbons increases during the second half of the plume's chemical lifetime, after the more reactive NMNIHC have been depleted. We estimate that during the

period when most of the O_3 is produced (i.e., time >4 hours), anthropogenic hydrocarbons contribute approximately 44%, biogenic hydrocarbons contribute 36%, and CO contribute 19% of the fuel for O_3 production in the urban plume.

In order to assess the full potential of VOC emission controls we must take into account the sum total of O_3 that such controls have the potential to affect. Consider, for example, the center of the mature urban plume on July 3 with a maximum of $\sim 115 \text{ ppbv}$ of O_3 . These 115 ppbv are apportioned as follows: $\sim 40 \text{ ppbv}$ represent the persistent background of a typical remote troposphere, 35 ppbv were generated by emissions from the Nashville urban plume, and 40 ppbv were produced by local and distant anthropogenic NO_x sources (see Table 9, background column). In total (Table 9, last column), 75 ppbv of O_3 can be attributed to anthropogenic NO_x emissions while utilizing 34% NMNIHC, 19% CO, and 45% biogenic hydrocarbons (isoprene, MAC, MVK, and HCHO). This estimate is consistent with the model calculations presented by Sillman *et al.* [1998].

5. Summary

Significant quantities of NO_x , CO, and reactive hydrocarbons are emitted from mobile and industrial sources in the Nashville urban area. The seven power plants surrounding Nashville emit NO_x continuously. This environment produces a high and persistent background of O_3 and related photochemical pollutants. Above this persistent high background, fresh emissions from the urban center form a well-defined plume in which additional O_3 is rapidly produced. For the 2 days examined here (July 3 and 18), the urban plume produced O_3 at a maximum rate of $\sim 10 \text{ ppbv per hour}$ with an efficiency of 2.5 to 4 O_3 per NO_x emitted. This plume consumed about half its NO_x and half its supply of anthropogenic hydrocarbons within 2 hours. This processing rate is consistent with an OH concentration of $\sim 1.2 \times 10^7 \text{ molecules cm}^{-3}$. The data also show that HNO_3 is rapidly removed from the system by dry deposition at a rate of $\sim 5 \text{ cm s}^{-1}$.

Hydrocarbon samples exhibited high and low isoprene concentrations. The isoprene concentrations observed in the urban plume were typically in the low regime. Even under these conditions, biogenic sources still contributed 36% of the hydrocarbons consumed for the production of O_3 in the urban plume, while anthropogenic hydrocarbons (NMNIHC) contributed 44% to ozone production in the urban plume (i.e., above background). It is concluded that further control of anthropogenic hydrocarbons would have only a limited effect on O_3 concentrations in the Nashville area.

Acknowledgments. The authors gratefully acknowledge a job well done by the ground and flight crews of all the research aircraft associated with SOS. Thanks to Ken Olszyna, Jim Pearson, and Tim Starn for providing data from the ground sites at Nashville. Thanks to Gerd Hübner for providing O_3 and CO data from the NOAA-AL WP-3D Orion. Also thanks to William Parkhurst for providing flight maps for the aircraft. The contributions of Paul Klotz are gratefully acknowledged. We would also like to thank the personnel at Signature Flight Support for their hospitality and assistance. This study was supported by funds the DOE Atmospheric Chemistry Program and from EPA through the SOS program. This paper has been authored under contract DE-AC02-98CH10886 with the Department of Energy. Accordingly, the U.S. Government retains a nonexclusive, royalty free license to publish or reproduce the published form of this contribution or to allow others to do so, for U.S. Government purposes.

References

- Apel, E.C., J.G. Calvert, R. Zika, M.O. Rodgers, V.P. Aneja, J.F. Meagher, and W.A. Lonneman, Hydrocarbon measurements during the 1992 southern oxidants study Atlanta Intensive: protocol and quality assurance, *J. Air Waste Manage. Assoc.*, **45**, 521-528, 1995.
- Chameides, W.L., and E.B. Cowling, The state of the southern oxidant study: Policy-relevant findings in ozone pollution research 1988-1994, report, U. S. EPA, Raleigh, North Carolina, April 1995.
- Chameides, W.L., et al., Ozone precursor relationships in the ambient atmosphere, *J. Geophys. Res.*, **97**, 6037-6055, 1992.
- Chameides, W.L., R.W. Lindsay, J. Richardson, and C.S. Kiang, The role of biogenic hydrocarbons in urban photochemical smog: Atlanta as a case study, *Science*, **241**, 6037-6055, 1988.
- Daum, P.H., L.I. Kleinman, L. Newman, W.T. Luke, J. Weinstein-Lloyd, C.M. Berkowitz, and K.M. Busness, Chemical and physical properties of anthropogenic pollutants transported over the North Atlantic during NARE, *J. Geophys. Res.*, **101**, 29,029-29,042, 1996.
- Dickerson, R.R., and A.C. Delany, Modification of a commercial gas filter correlation CO detector for enhanced sensitivity, *J. Atmos. Oceanic. Technol.*, **5**, 424-431, 1988.
- Duncan, B.N., A.W. Stelson, and C.S. Kiang, Estimated contribution of power plants to ambient nitrogen oxides measured in Atlanta, Georgia in August 1992, *Atmos. Environ.*, **29**, 3043-3054, 1995.
- Fehsenfeld, F.C., et al., A ground-based intercomparison of NO, NO_x, and NO_y measurement techniques, *J. Geophys. Res.*, **92**, 14,710-14,722, 1987.
- Finlayson-Pitts, B.J., and J.N. Pitts Jr., *Atmospheric Chemistry: Fundamentals and Experimental Techniques*, p. 532, John Wiley, New York, 1986.
- Goldan, P.D., W.C. Kuster, and F.C. Fehsenfeld, The relative importance of isoprene and anthropogenic nonmethane hydrocarbons on ozone production in the southeastern United States, (abstract), *Eos Trans. AGU*, **77**(46), Fall Meet. Suppl., F82, 1996.
- Hall, B.D., and C.S. Claiborne, Measurements of the dry deposition of peroxides to a Canadian boreal forest, *J. Geophys. Res.*, **102**, 29,343-29,353, 1997.
- Hildebrand, P.H., and B. Ackerman, Urban effects on the convective boundary layer, *J. Atmos. Sci.*, **41**, 76-91, 1984.
- Holdren, M.W. and C.W. Spicer, Field compatible calibration procedure for peroxyacetyl nitrate, *Environ. Sci. Technol.*, **18**, 113-116, 1984.
- Hübner, G., et al., An overview of the airborne activities during the SOS 1995 Nashville/Middle Tennessee Ozone Study, *J. Geophys. Res.*, in press, 1998.
- Huebert, B.J., and C.H. Robert, The dry deposition of nitric acid to grass, *J. Geophys. Res.*, **90**, 2085-2090, 1985.
- Joos, E., B. Millancourt, H. van Durren, and F.G. Romer, Physicochemical study by two aircraft of a plume from a coal-fired power plant, *Atmos. Environ.*, **24a**, 703-710, 1990.
- Keiser, B., and V. Young, Southern Oxidant Study 1996: Hydrocarbon analysis, report, Cent. for Atmos. Chem., York Univ., North York, Ontario, Canada, 1996.
- Kleinman, L., et al., Ozone formation at a rural site in the southeastern United States, *J. Geophys. Res.*, **99**, 3469-3482, 1994.
- Kleinman, L.I., P. H. Daum, D.G. Imre, C. Cardelino, K.J. Olszyna, and R.G. Zika, Trace gas concentrations and emissions in downtown Nashville during the 1995 SOS/Nashville Intensive, *J. Geophys. Res.*, in press, 1998.
- Leahy, D.F., P.J. Klotz, S.R. Springston, and P.H. Daum, The Brookhaven National Laboratory filter pack sampling system for collection and determination of air pollutants, *Rep. BNL-61730*, Brookhaven Natl. Lab., Upton, New York, 1995.
- Lee, J.H., I.N. Tang, and J. Weinstein Lloyd, Nonenzymatic method for the determination of hydrogen peroxide in atmospheric samples, *Anal. Chem.*, **62**, 2381-2384, 1990.
- Lee, J.H., D.F. Leahy, I.N. Tang, and L. Newman, Measurement and speciation of gas-phase peroxides in the atmosphere, *J. Geophys. Res.*, **98**, 2911-2915, 1993.
- Lee, J.H., I.N. Tang, J. Weinstein-Lloyd, and E. Halper, An improved nonenzymatic method for determination of gas-phase peroxides, *Environ. Sci. Technol.*, **28**, 1180-1185, 1994.
- Lee, Y.-N. and X. Zhou, Method for the determination of some soluble atmospheric carbonyl compounds, *Environ. Sci. Technol.*, **27**, 749-756, 1993.
- Lee, Y.-N., X. Zhou, W.R. Leitch, and C.M. Banic, An aircraft measurement technique for formaldehyde and soluble carbonyl compounds, *J. Geophys. Res.*, **101**, 29,075-29,080, 1996.
- Lee, Y.-N., et al., Atmospheric chemistry and distribution of formaldehyde and several multi-oxygenated carbonyl compounds during the 1995 Nashville/Middle Tennessee Ozone Study, *J. Geophys. Res.*, in press, 1998.
- Meagher, J.F., W.J. Parkhurst, and J.L. Christ, The SOS Nashville/Middle Tennessee Ozone Field Study data base, Environ. Res. Cent., Tenn. Val. Auth., Muscle Shoals, Ala., 1996.
- National Academy of Sciences, *Rethinking the Ozone Problem in Urban and Regional Air Pollution*, Nat. Acad., Washington, D. C., 1991.
- Olszyna, K.J., E.M. Bailey, R. Simonaitis, and J.F. Meagher, O₃ and NO_y relationships at a rural site, *J. Geophys. Res.*, **99**, 14,557-14,563, 1994.
- Parrish, D.D., M. Trainer, M.P. Buhr, B.A. Watkins, and F.C. Fehsenfeld, Carbon monoxide concentrations and their relation to concentrations of total reactive oxidized nitrogen at two rural U.S. sites, *J. Geophys. Res.*, **96**, 9309-9320, 1991.
- Sillman, S., Tropospheric ozone: The debate over control strategies., *Annu. Rev. Energy Environ.*, **18**, 31-56, 1993.
- Sillman, S., D. He, M.R. Pippen, P.H. Daum, D.G. Imre, J.H. Lee, L.I. Kleinman, and J. Weinstein-Lloyd, Model correlations for ozone, reactive nitrogen and peroxides for Nashville in comparison with measurements: Implications for O₃-NO_x-hydrocarbon chemistry, *J. Geophys. Res.*, in press, 1998.
- Spangler, T.C., and R.A. Dirks, Meso-scale variations of the urban mixing height, *Boundary Layer Meteorol.*, **6**, 423-441, 1974.
- Trainer, M., et al., Correlation of ozone with NO_y in photochemically aged air, *J. Geophys. Res.*, **98**, 2917-2925, 1993.
- Trainer, M., B.A. Ridley, M.P. Buhr, G. Kok, J. Walega, G. Hübner, D.D. Parrish, and F.C. Fehsenfeld, Regional ozone and urban plumes in the southeastern United States: Birmingham, a case study, *J. Geophys. Res.*, **100**, 18,823-18,834, 1995.
- Watkins, B.A., D.D. Parish, M. Trainer, R.B. Norton, J.E. Yee, F.C. Fehsenfeld, and B.G. Heikes, Factors influencing the concentration of gas phase hydrogen peroxide during the summer at Niwot Ridge, Colorado, *J. Geophys. Res.*, **100**, 22,831-22,840, 1995.
- Weinstein-Lloyd, J.B., J.H. Lee, P.H. Daum, L.I. Kleinman, L.J. Nunnermacker, S.R. Springston, and L. Newman, Measurements of peroxides and related species during the 1995 summer intensive of the Southern Oxidants Study in Nashville, Tennessee, *J. Geophys. Res.*, in press, 1998.
- Williams, E.J., et al., Intercomparison of NO_y measurement techniques, *J. Geophys. Res.*, in press, 1998.
- R. Alvarez, R. Banta, and C. Senff, NOAA-Environmental Resources Laboratory, Boulder, CO 80307.
- P.H. Daum, D. Imre, L. Kleinman, J. H. Lee, Y.-N. Lee, L. Newman, L. J. Nunnermacker, and S. R. Springston, Environmental Chemistry Division, Department of Applied Science, Brookhaven National Laboratory, P.O. Box 5000, Upton, NY 11973-5000. (e-mail: lindan@bnl.gov.)
- M. Holdren and G. W. Keigley, Atmospheric Science and Applied Technology, Battelle-Columbus, Columbus, OH 43201.
- W. T. Luke, NOAA-Air Resources Laboratory, Silver Spring, MD 48109.
- S. Sillman, Department of Atmospheric, Oceanic and Space Sciences, University of Michigan, Ann Arbor, MI 48109.
- J. Weinstein-Lloyd, Chemistry/Physics Department, SUNY, Old Westbury, NY 11568.
- X. Zhou, New York State Department of Health, Albany, NY 12201.

Table 1. Average O₃ and CO Concentrations Obtained by the NOAA-AL WP-3D Orion on July 3

Location	Altitude, m	Average [O ₃] ± s.d.	Average [CO] ± s.d.
South of Nashville	400	72 ± 4	300 ± 23
South of Nashville	600	78 ± 9	280 ± 19
South of Nashville	900	69 ± 1	268 ± 5
North of Nashville	400	55 ± 7	276 ± 17
North of Nashville	600	65 ± 17	290 ± 19
North of Nashville	900	71 ± 12	280 ± 11
NE of Nashville	525	74 ± 3	280 ± 10
NE of Nashville	900	75 ± 9	311 ± 40

Concentrations in ppbv. Abbreviation s.d., standard deviation.

Table 2. Average Background Concentrations Upwind of Nashville (DOE G-1) on July 3

Altitude, m	O ₃	CO	SO ₂	NO _x	NO _y
600	72 ± 4	310 ± 30	1.7 ± 1	0.40 ± 0.25	5.4 ± 0.4
1200	71 ± 4	305 ± 16	1.2 ± 0.6	0.42 ± 0.60	5.4 ± 0.5
1800	56 ± 2	181 ± 18	0.02 ± 0.12	DL	2.4 ± 0.3

Concentrations in ppbv. Abbreviation DL, detection limit.

Table 3. Average Hydrocarbon Concentrations for July 3, 1995

Location	n	Isoprene Regime	[NMNIHC] ± s.d.	[CO] ± s.d.	[Isoprene] ± s.d.	[HCHO] ± s.d.
Upwind	2	low	12.2 ± 0.7	296 ± 28	1.0 ± 0.6	3.0 ± 0.9
Upwind	4	high	20.0 ± 9.8	345 ± 13	6.1 ± 2.1	4.9 ± 0.7
DW1	6	low	19.0 ± 3.7	354 ± 39	1.0 ± 0.2	3.8 ± 0.8
DW2	1	low	26.2 ± (NA)	453 ± (NA)	0.84 ± (NA)	4.8 ± (NA)
Downtown	1	low	243 ± (NA)	1200 ± (NA)	0	NA

Samples obtained in boundary layer (i.e., altitude <1300 m). Concentrations in ppb C
Abbreviations s.d., standard deviation; NA, not applicable

Table 4. Maximum Concentrations Above Background for Trace Gases in the Urban Plume on July 3, 1995

Location	Altitude, m	[O ₃]	[CO]	[NO _x]	[NO _y]
DW1	500	31 ± 3	NA	1.4 ± 0.3	7.5 ± 0.7
DW2	500	35 ± 3	159 ± 20	1.3 ± 0.3	6.7 ± 0.6
DW1	1200	28 ± 3	103 ± 15	0.8 ± 0.3	5.8 ± 0.6
DW2	1200	33 ± 3	106 ± 15	0.8 ± 0.4	6.0 ± 0.6

Concentrations in ppbv. NA, not applicable

Table 5. Average Hydrocarbon Concentrations for July 18, 1995

Location	n	Isoprene	[NMNIHC] \pm s.d.	[CO] \pm s.d.	[Isoprene] \pm s.d.	[HCHO] \pm s.d.
		Regime				
Upwind	7	Low	20.6 \pm 11	145 \pm 6	1.0 \pm 0.6	1.6 \pm 0.1
EW1	5	Low	15.0 \pm 3.6	181 \pm 27	0.68 \pm 0.3	2.6 \pm 0.4
EW2	2	Low	11.0 \pm 1.5	185 \pm 10	0.43 \pm 0.02	2.9 \pm 0.1
EW2	1	High	10.1 \pm (NA)	188 \pm (NA)	7.3 \pm (NA)	2.9 \pm (NA)
Downtown	1	Low	75.0 \pm (NA)	400 \pm (NA)	1.4 \pm (NA)	Not measured

Samples obtained in boundary layer (i.e., altitude <1300 m). Concentrations in ppb C Abbreviations s.d., standard deviation; NA, not applicable

Table 6. Average Background Concentrations North of Nashville on (DOE G-1) July 18, 1995

Altitude, m	O ₃	CO	SO ₂	NO _x	NO _y
300	60 \pm 2	145 \pm 13	3.7 \pm 1.0	1.0 \pm 0.6	4.1 \pm 0.9
500	58 \pm 2	150 \pm 13	3.2 \pm 1.8	1.1 \pm 0.7	3.8 \pm 1.0
630	62 \pm 2	143 \pm 10	3.1 \pm 1.0	0.8 \pm 0.8	3.8 \pm 1.0

Concentrations in ppbv

Table 7. Maximum Concentrations Above Background of Trace Gases in the Urban Plume on July 18, 1995

Location	Altitude, m	[O ₃]	[CO]	[NO _x]	[NO _y]
Downtown	150	10 \pm 2	150 \pm 15	NA	15 \pm 2
EW1	630	14 \pm 2	100 \pm 15	6.5 \pm 1	10 \pm 2
NS	630	12 \pm 2	60 \pm 20	1.0 \pm 0.3	3 \pm 0.3

Concentrations in ppbv. NA, not applicable.

Table 8. Elapsed Time From Point of Emission to Point of Sampling Urban Plume

Date	Location	Time, hours
July 18, 1995	EW1	2.0
July 18, 1995	NS	4.0
July 3, 1995	DW1	4.5
July 3, 1995	DW2	7.0

Table 9. Estimated Percent Contribution of Anthropogenic and Biogenic Hydrocarbons to O₃ Production in the Center of the Urban Plume

Hydrocarbon	Urban Plume (First 2 hours)	Urban Plume	Background	Total
CO	19	19	20	19
NMNIHC	55	44	25	34
Isoprene + MVK + MAC	14	25	40	34
HCHO	11	11	11	11
CH ₄	1.5	2.5	4	3
[O ₃] _{produced} (ppbv)	20.5	35	40	75

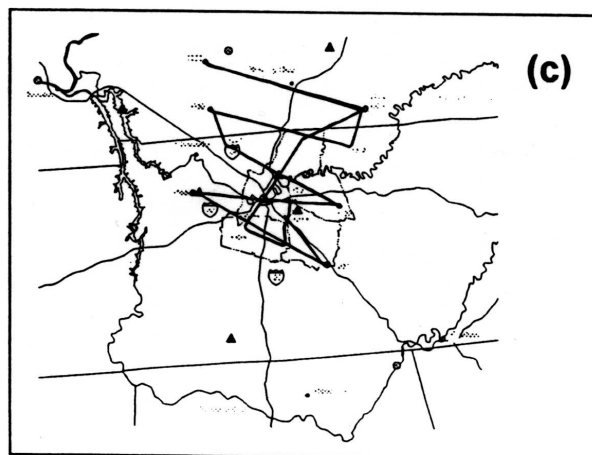
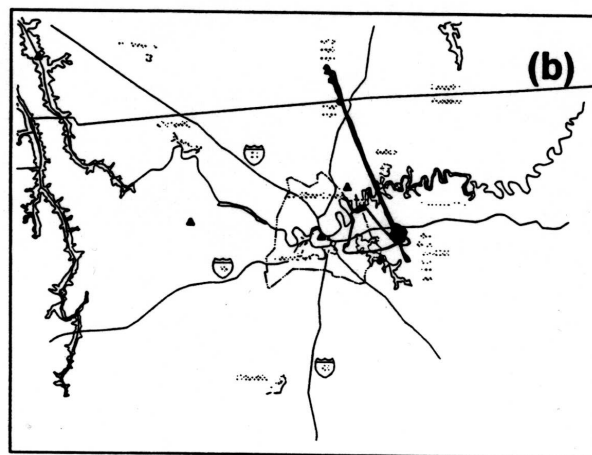
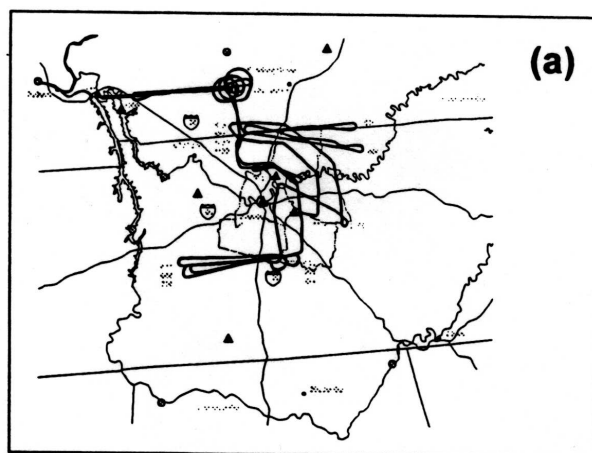


Figure 1. Flight tracks of (a) NOAA-AL WP-3D Orion, (b) NOAA-ARL Twin Otter, and (c) NOAA-ERL CASA 211 on July 3, 1995.

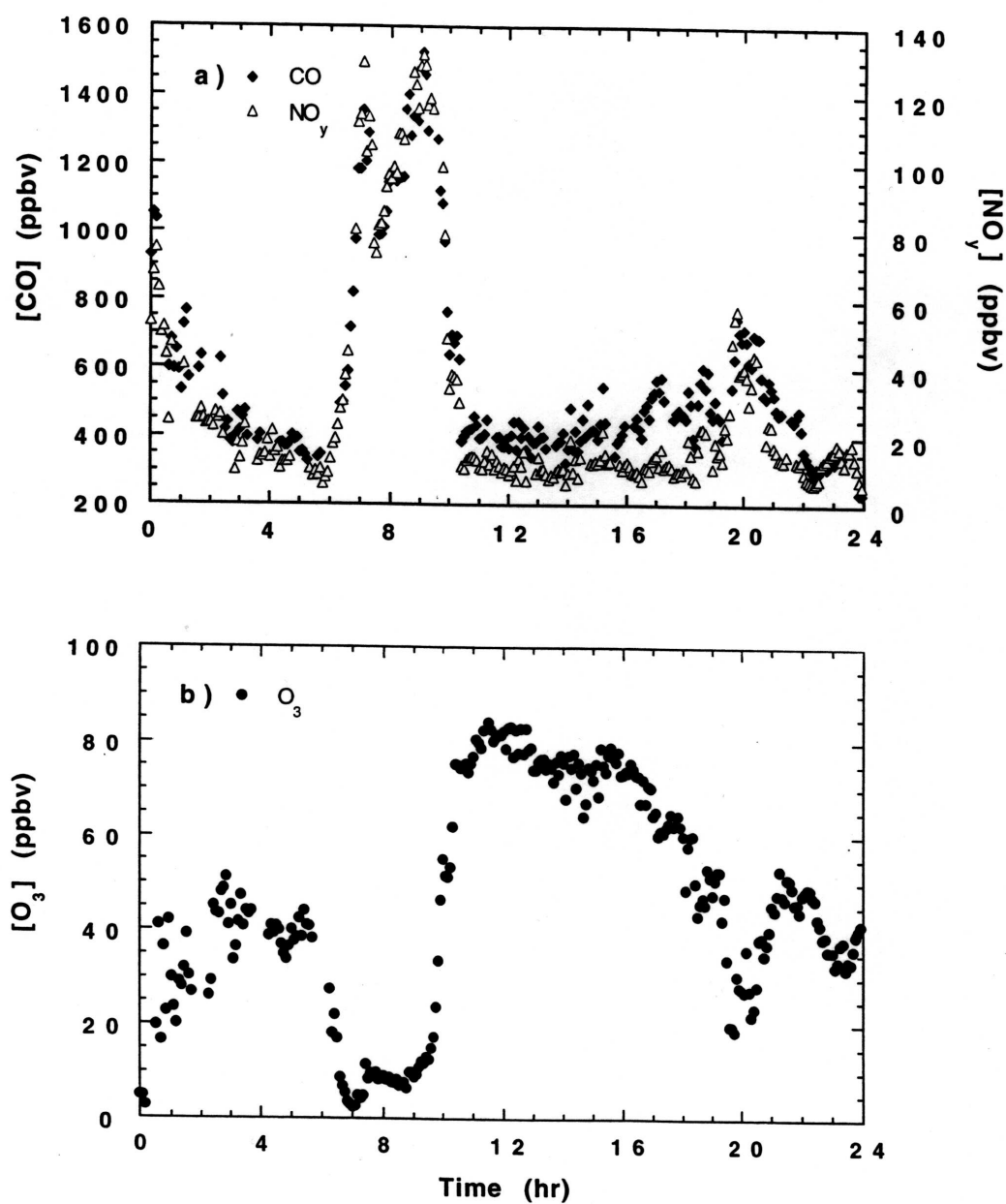


Figure 2. Measurements of (a) CO, NO_y and (b) O₃ made at the downtown Nashville monitoring site on July 3, 1995. Note the correlation between CO and NO_y and the sharp break up of the nocturnal boundary layer at 10:00. The effect of titration is clearly visible in the O₃ trace during the morning hours. A secondary increase in pollutant concentrations is evident at 20:00.

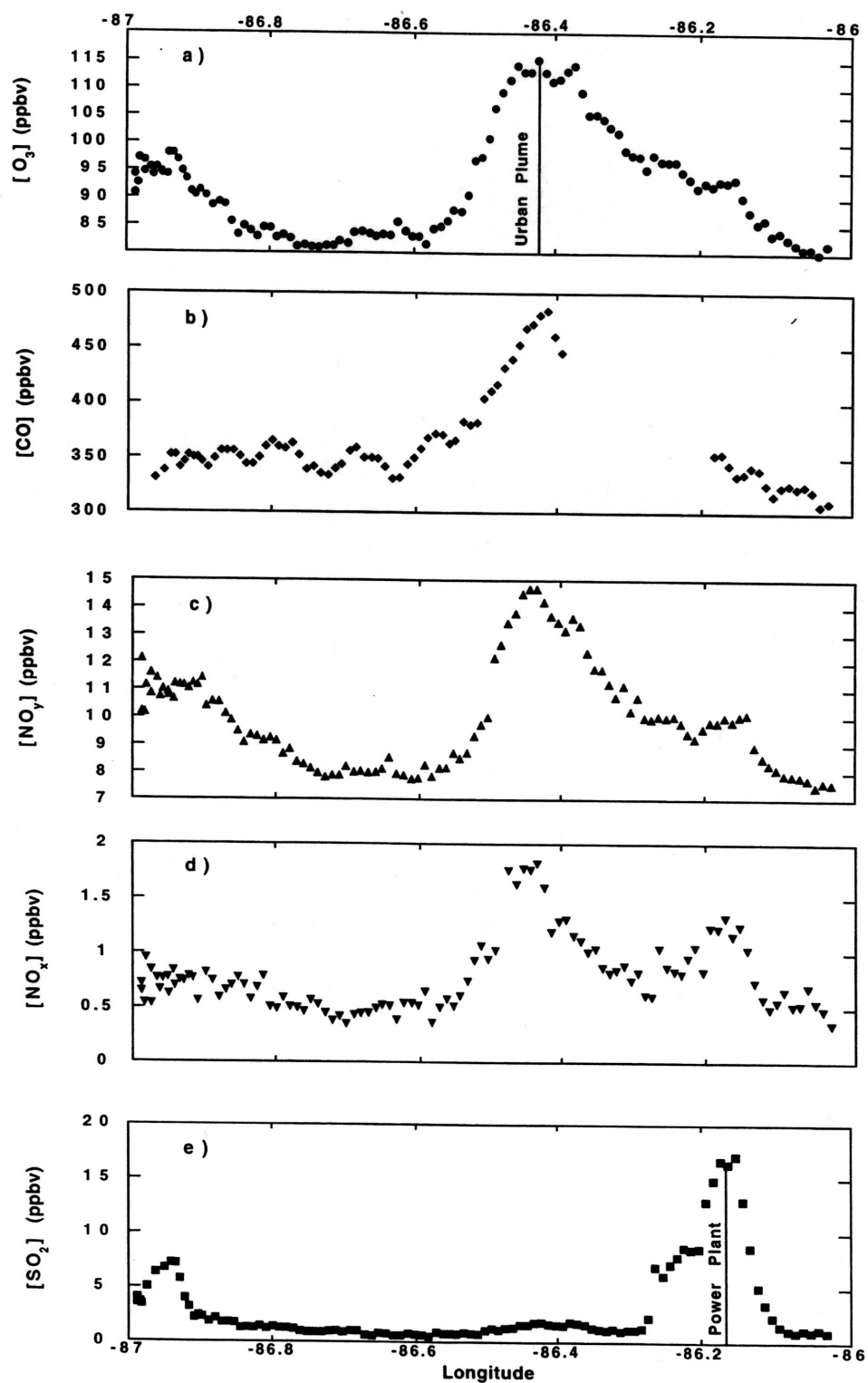


Figure 3. A typical example of trace gas concentrations obtained during a cross-plume transect (DW2) on July 3, 1995: (a) O_3 , (b) CO , (c) NO_y , (d) NO_x , and (e) SO_2 . The presence of the urban plume at -86.4° longitude is evident from the high CO concentrations. The Gallatin power plant plume, centered at -86.17° longitude, is associated with high SO_2 concentrations.

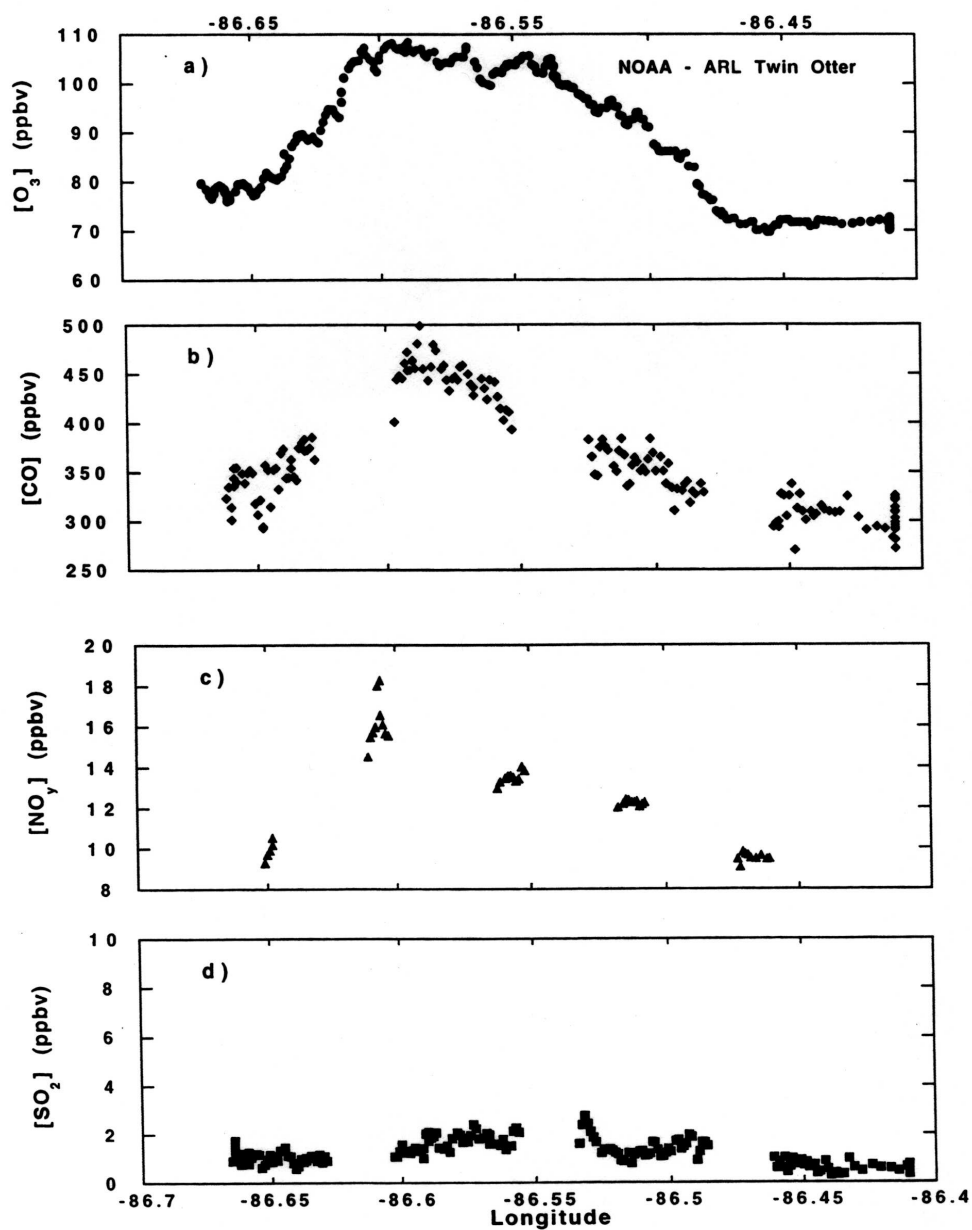


Figure 4. Similar to Figure 3 except that these data were obtained by the NOAA-ARL Twin Otter. The Gallatin power plant plume was not intercepted by the Twin Otter. Note the good agreement between the two measurement platforms.

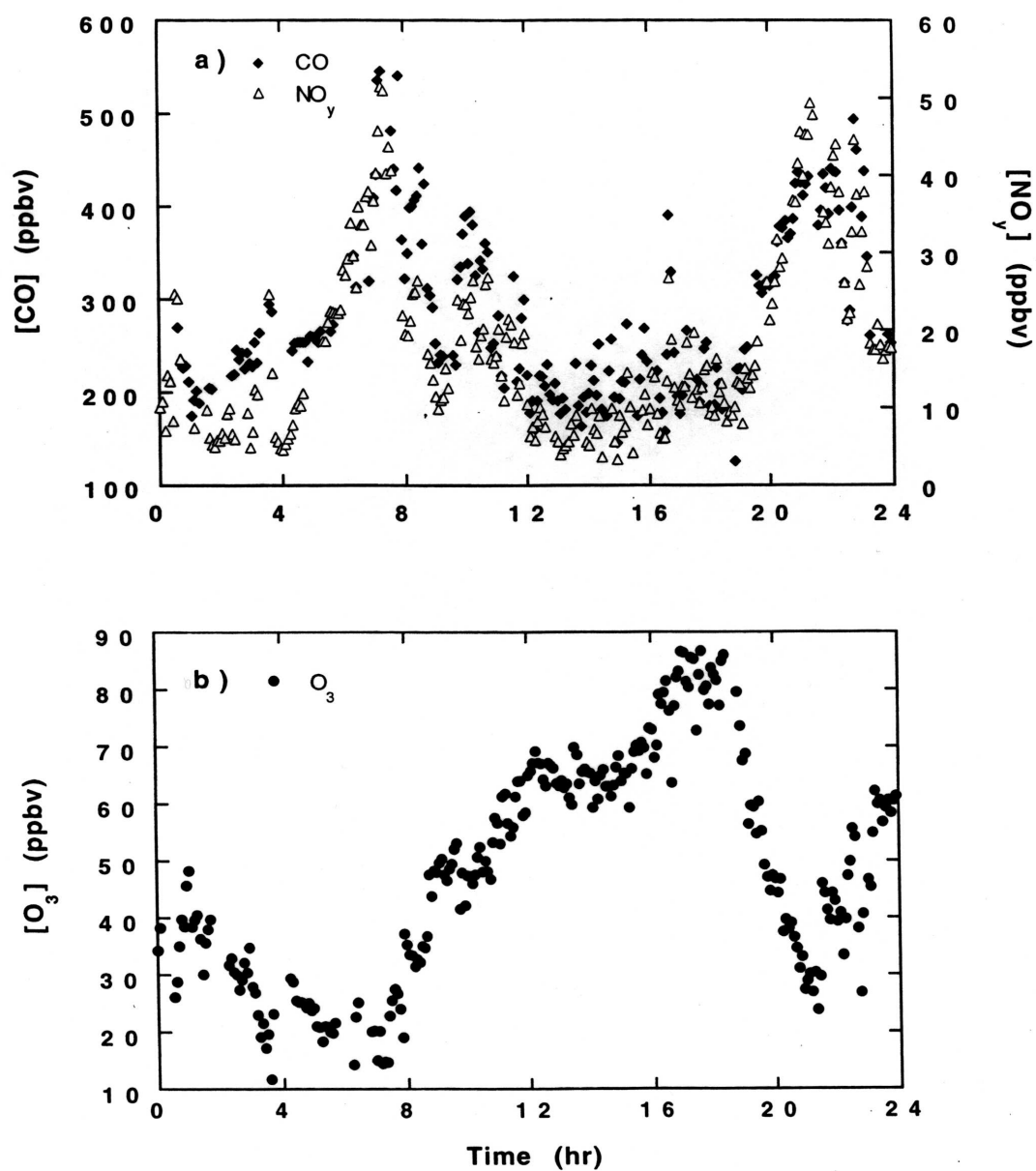


Figure 5. Measurements of (a) CO, NO_y and (b) O₃ made at the downtown Nashville monitoring site on July 18, 1995. The average pollutant concentrations on this day were lower than those observed on July 3, 1995, consistent with the higher wind speed.

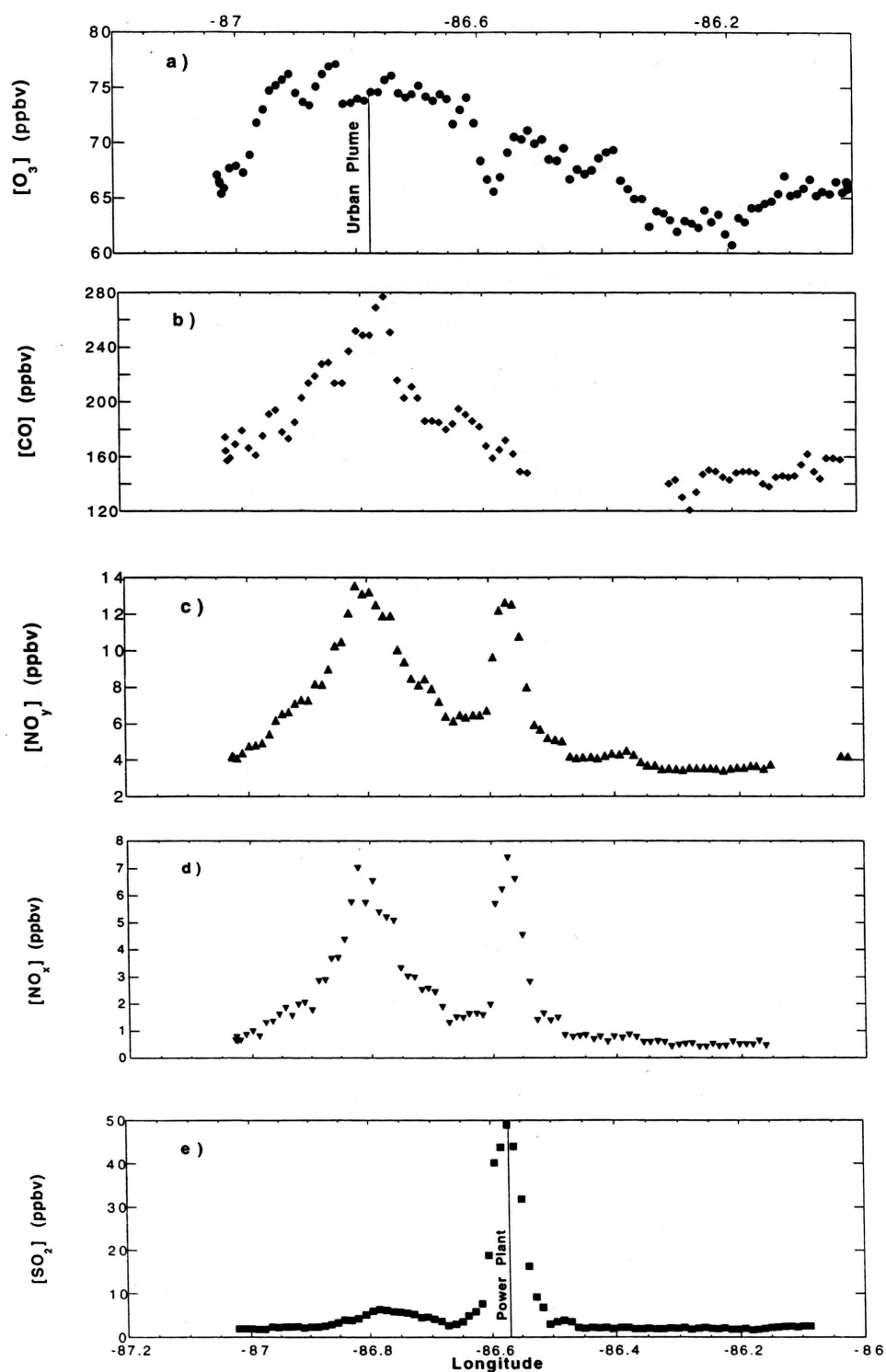


Figure 6. A typical example of trace gas concentrations obtained during one of the cross-plume transects (EW1) on July 18, 1995: (a) O_3 , (b) CO , (c) NO_y , (d) NO_x , and (e) SO_2 . The presence of the urban plume, centered at -86.8° longitude, is evident from the high CO concentrations. The Gallatin power plant plume, centered at -86.56° longitude is associated with high SO_2 concentrations.

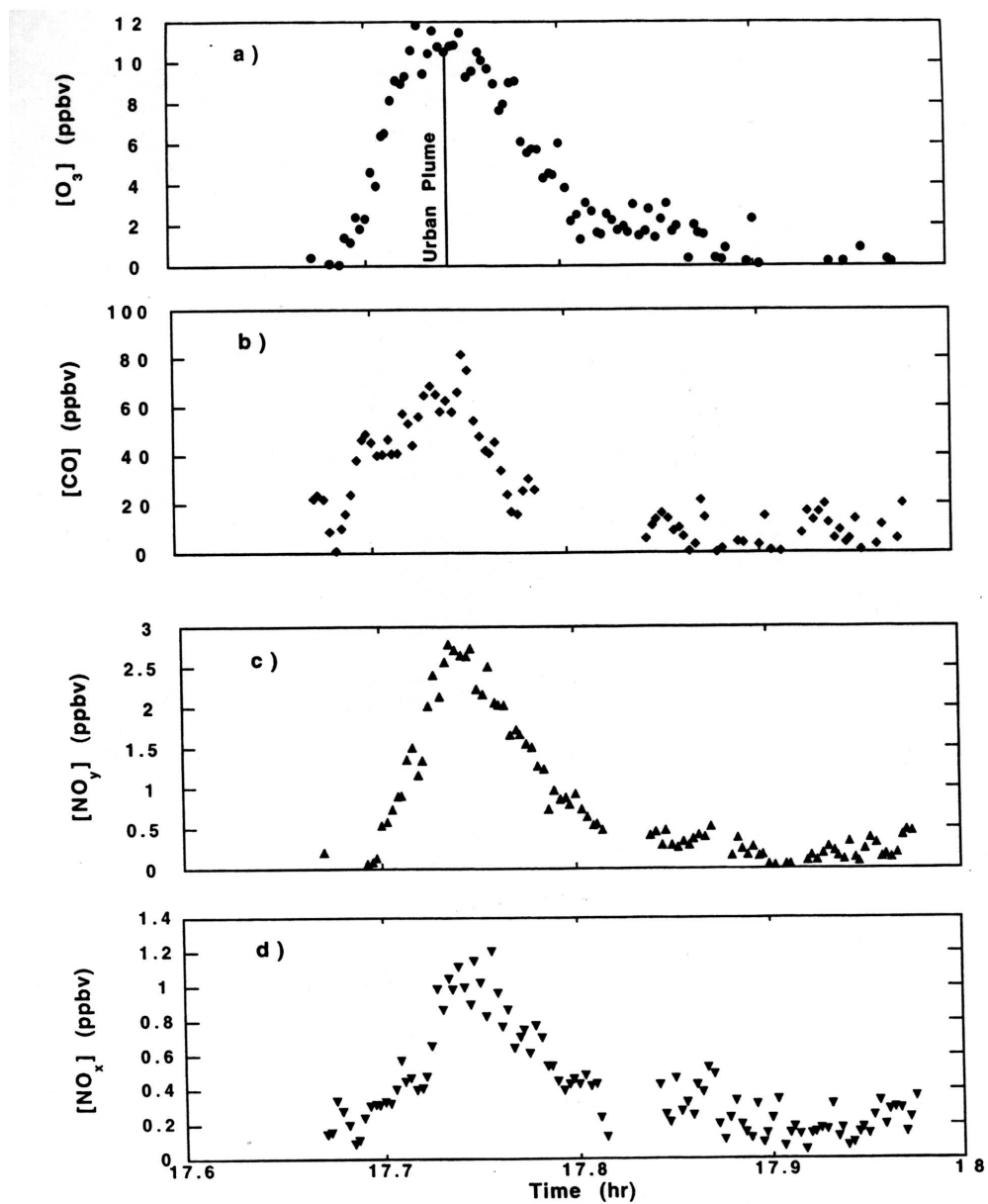


Figure 7. Trace gas concentrations obtained during the NS cross-plume transect on July 18, 1995: (a) O_3 , (b) CO , (c) NO_y , and (d) NO_x . Background concentrations have been subtracted.

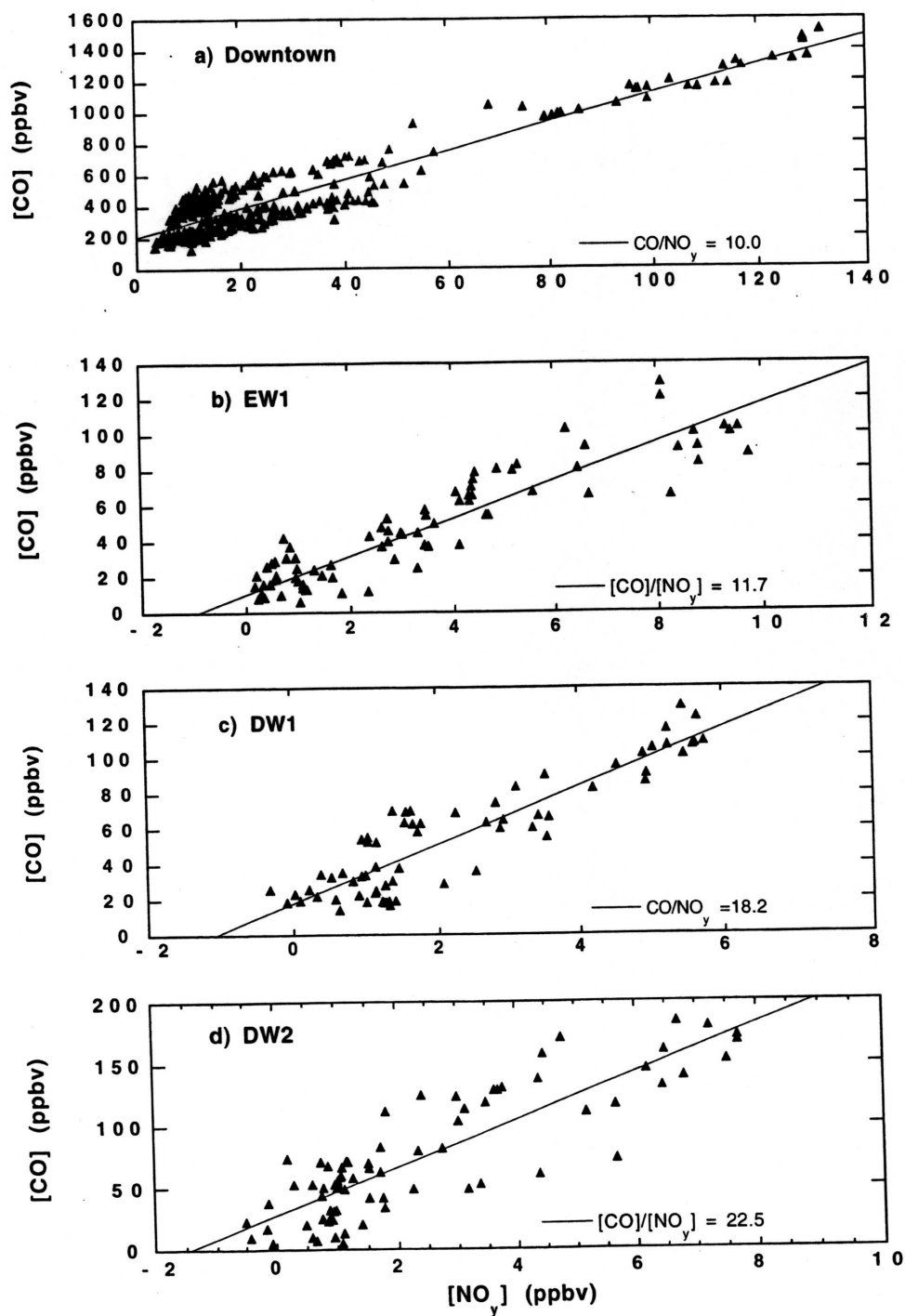


Figure 8. A study of the CO to NO_y relationship on July 3 and 18, 1995, for (a) Downtown-combined data for both days, (b) EW1-combined data from 500 and 630 m, (c) DW1-combined data from 600 and 1200 m, (d) DW2-combined data from 600 and 1200 m. Figures 8a to 8d are arranged in order of increasing processing times. The reported ratios were derived from the slopes of the linear regressions. Note the increasing CO/ NO_y ratio with processing time.

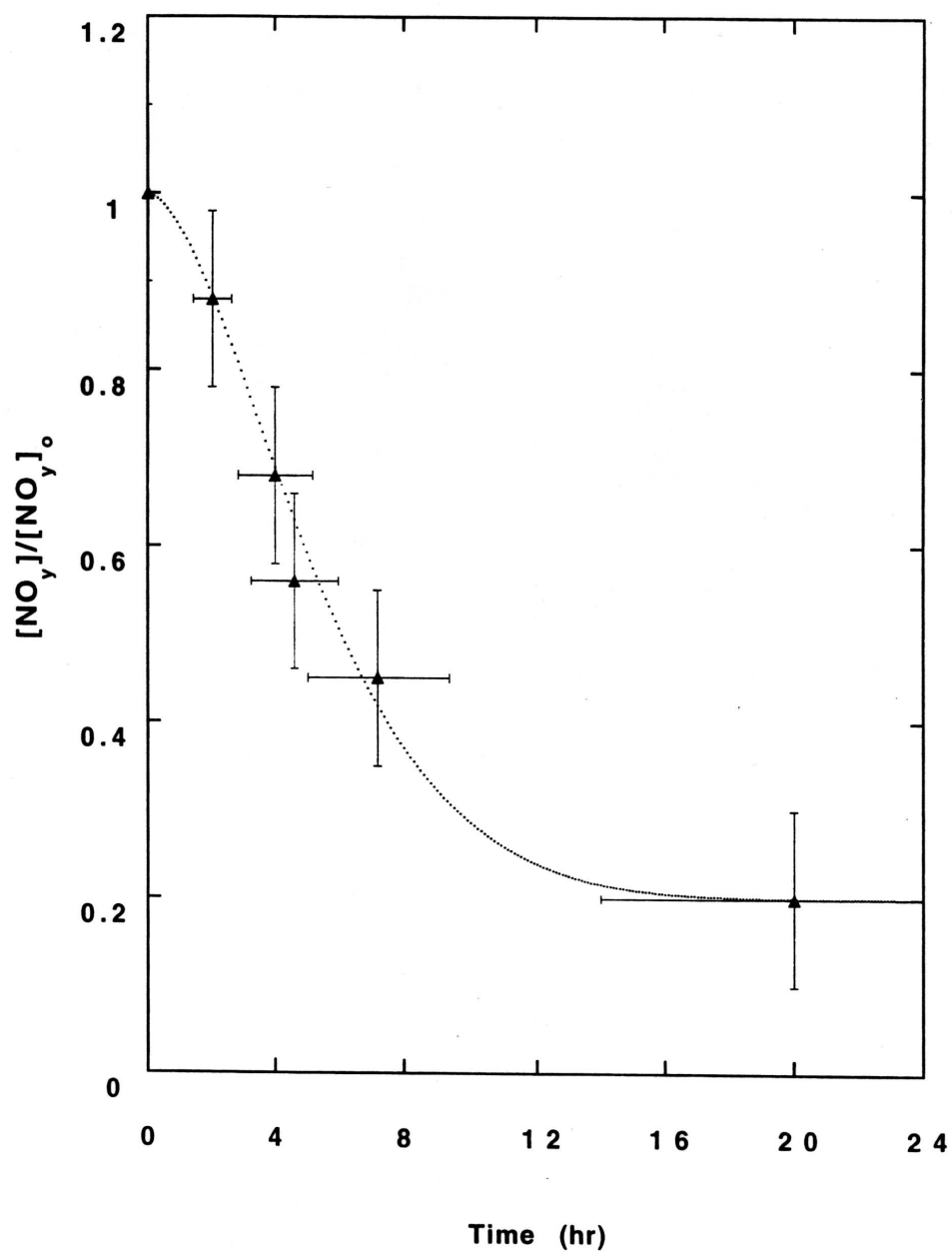


Figure 9. After correcting for NO_y losses based on the observations made in Figure 8, the ratio of $[NO_y]/[NO_y]_0$ is plotted as a function of time. The dotted line is a non-exponential qualitative fit to the data, with a NO_y phenomenological lifetime of 5.8 hours. Note that at long processing times the curve decays to 0.2, representing organic nitrates and NO_x.

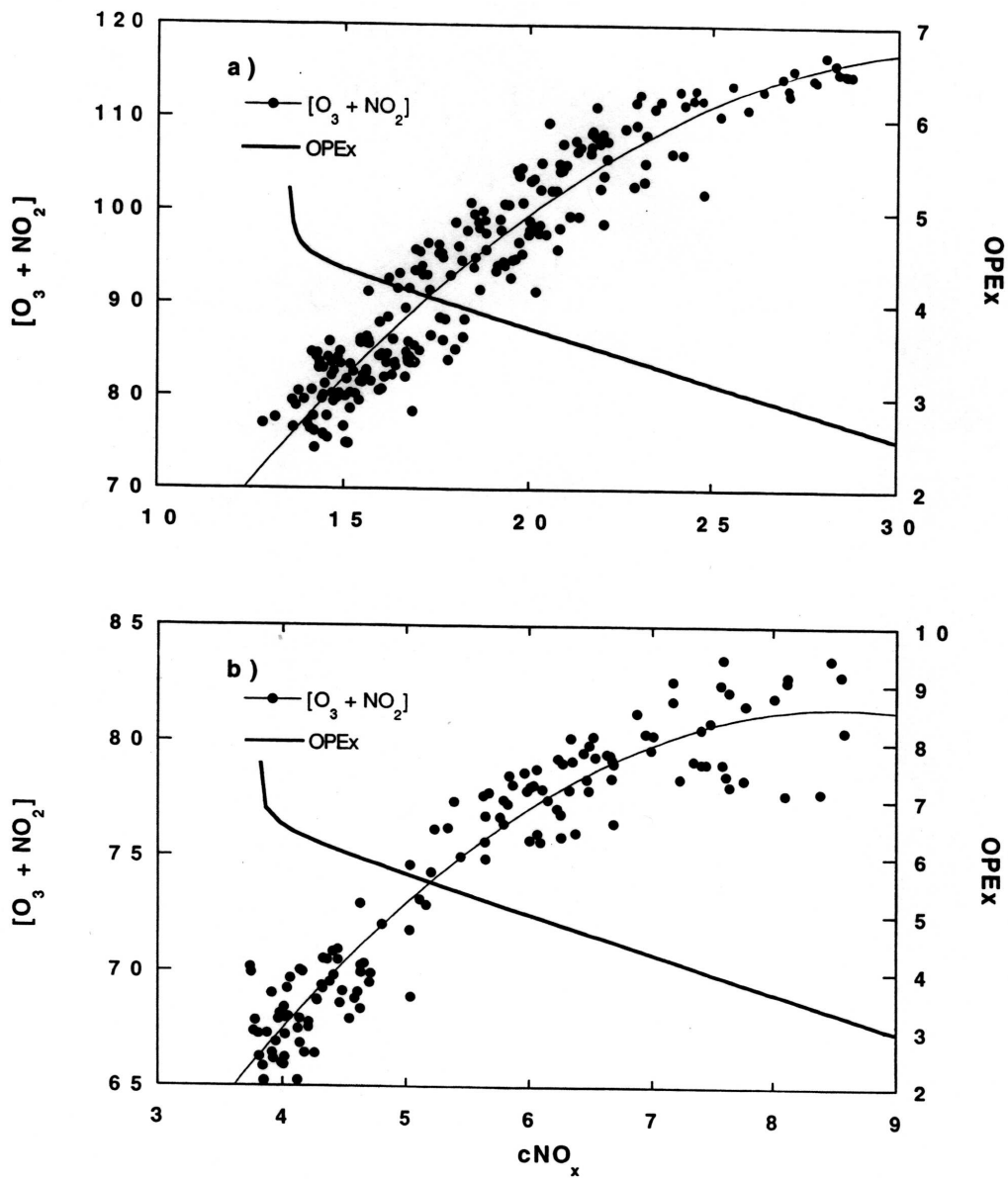


Figure 10. A study of the O₃ production efficiency (OPE_x) for the urban plume on (a) July 3 and (b) July 18 1995. The figure shows the observed oddO (O₃ + NO₂) plotted against consumed NO_x (cNO_x). A quadratic fit to the data is marked with a thin solid line. The second Y axis refers to the thick solid lines representing the calculated OPE_x, which was calculated according to (oddO-background)/(cNO_x-background). Note that the range of OPE_x in the two panels are not the same. The sharp rise in OPE_x at the edge of the plume is an artifact of a division of two small numbers.

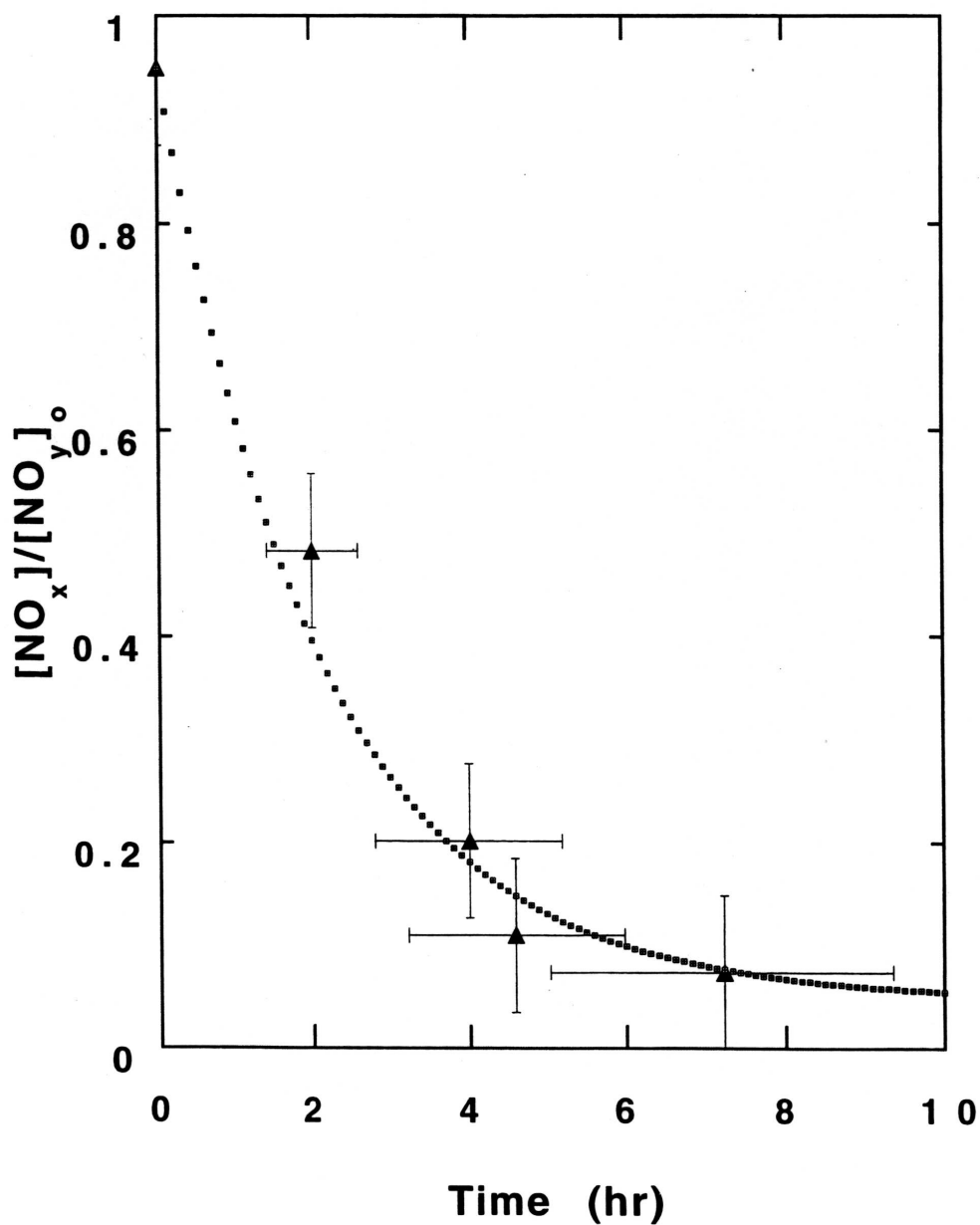


Figure 11. A study of the NO_x consumption rate: the data from July 3 (DW1 and DW2) and July 18 (EW1 and NS) in plots of NO_x versus [NO]_o. The latter quantity was derived by correcting for dry depositional losses in NO_y. Figures 11a to 11d are ordered according to increasing processing times. The reported ratios were obtained from the slopes of the linear regressions.

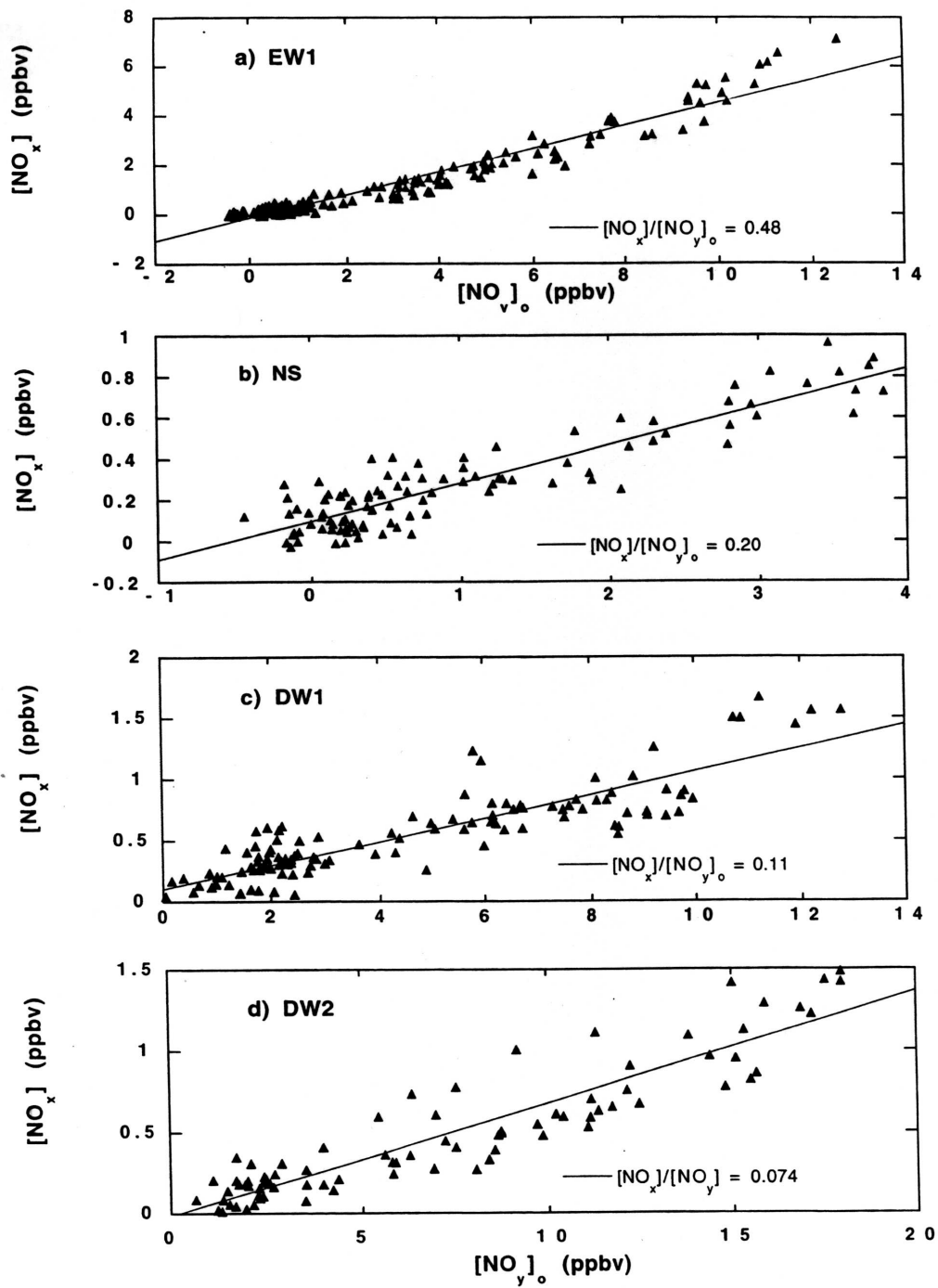


Figure 12. A plot of the ratio $[\text{NO}_x]/[\text{NO}_y]_o$, obtained from the regression slopes in Figure 11, as a function of time. The dotted line is a fit to the data with a $1/e$ lifetime of 2.1 hours.

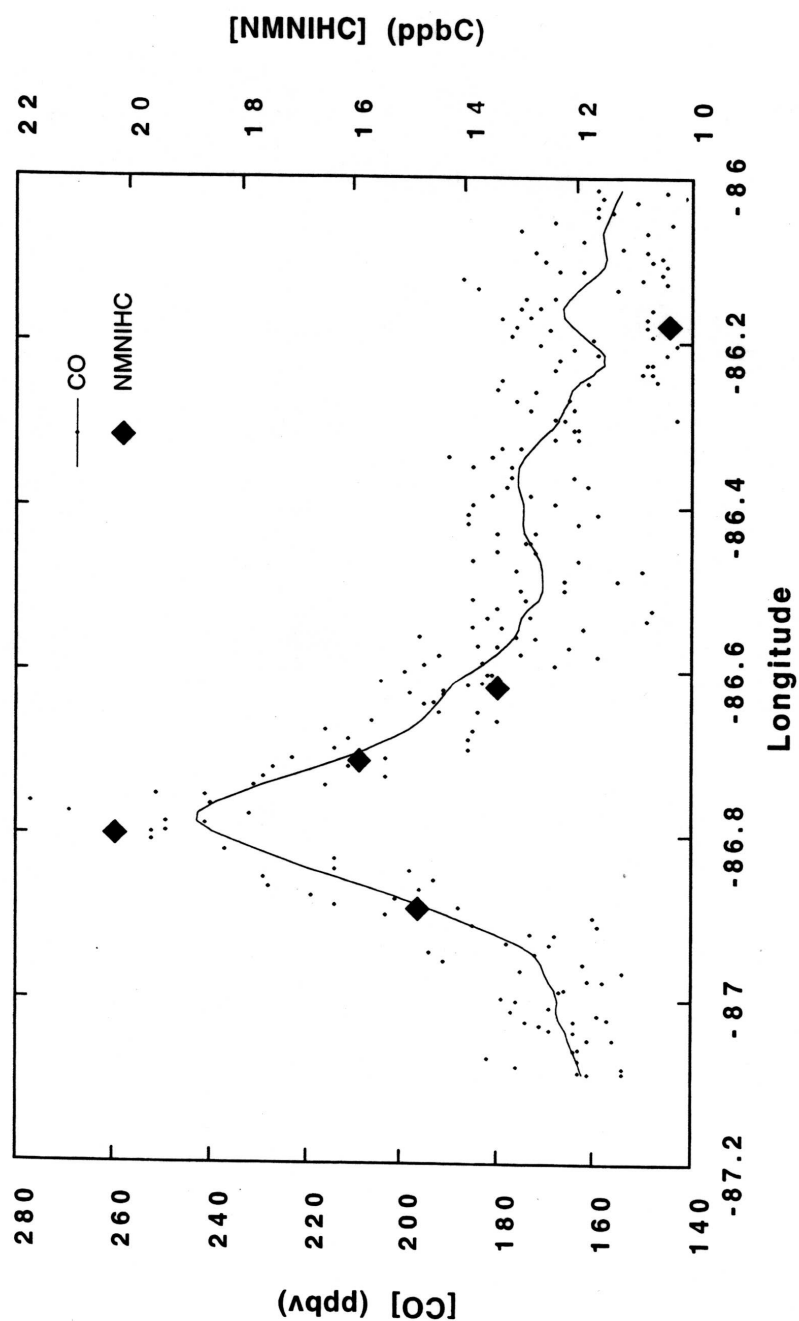


Figure 13. A plot of the sum of the anthropogenic hydrocarbons (NMNIHC) obtained from grab samples at three altitudes during the EW1 cross-plume transect on July 18, 1995. Also shown are the observed CO concentrations during these transects.

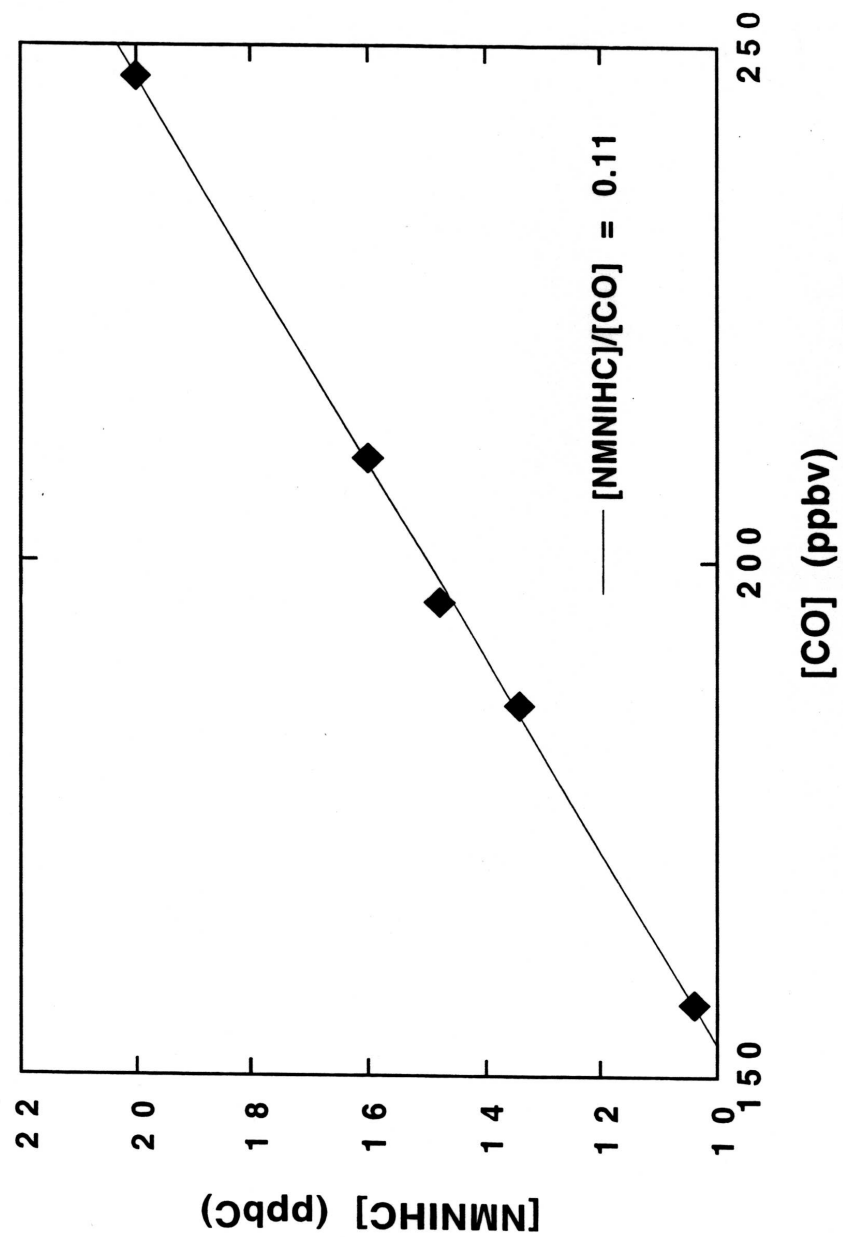


Figure 14. A linear regression of the [NMNIHC] versus [CO] data presented in Figure 13. The derived slope (0.11) indicates that more than 50% of the NMNIHC that were present downtown have been consumed within 2 hours.

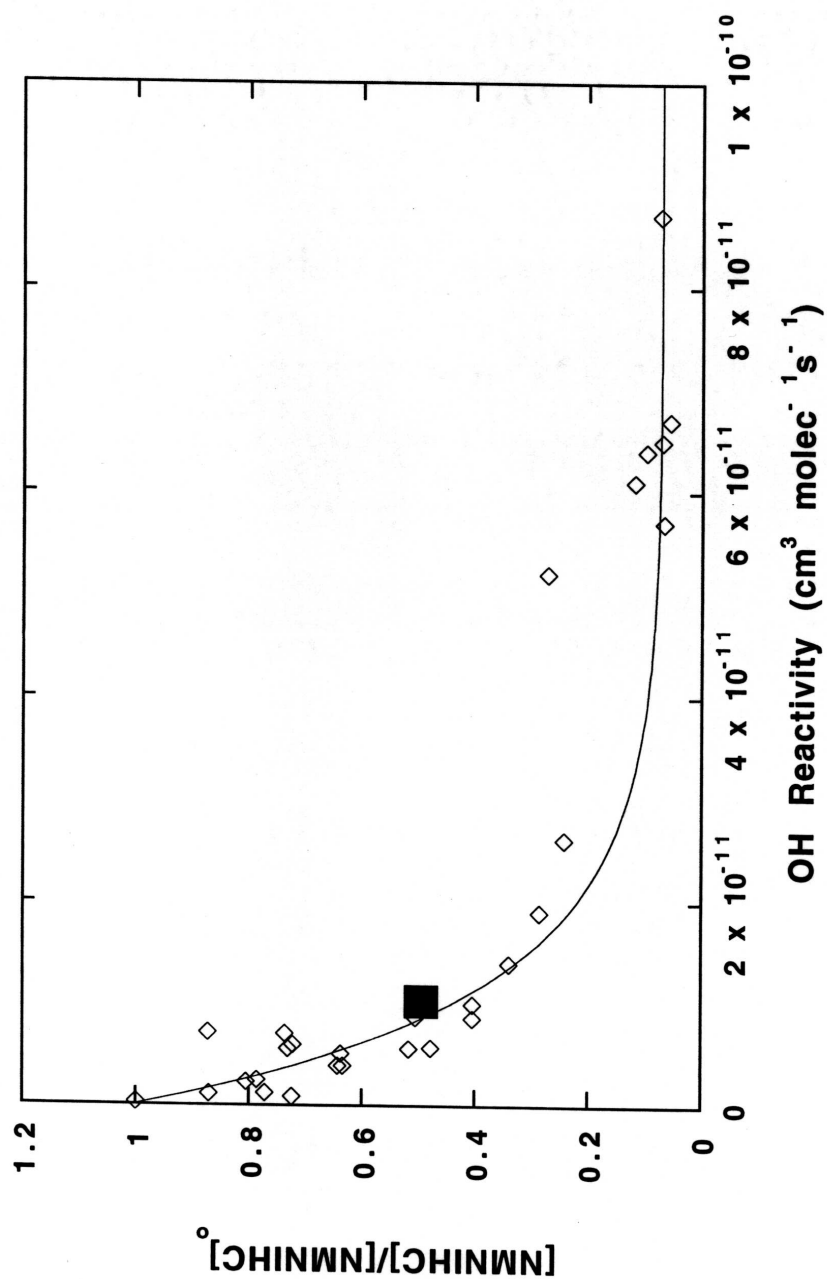


Figure 15. A study of the individual hydrocarbons observed during the EW1 transect on July 18 presented in a plot of each hydrocarbon's unreacted fraction ($[NMNIHC]/[NMNIHC]_0$) versus its rate constant (k) with OH. The solid line is the predicted exponential function assuming an OH concentration of 1.15×10^7 molecules cm^{-3} . Also shown in the figure, black square, is the observed fraction of unreacted NO_2 and its rate constant with OH.

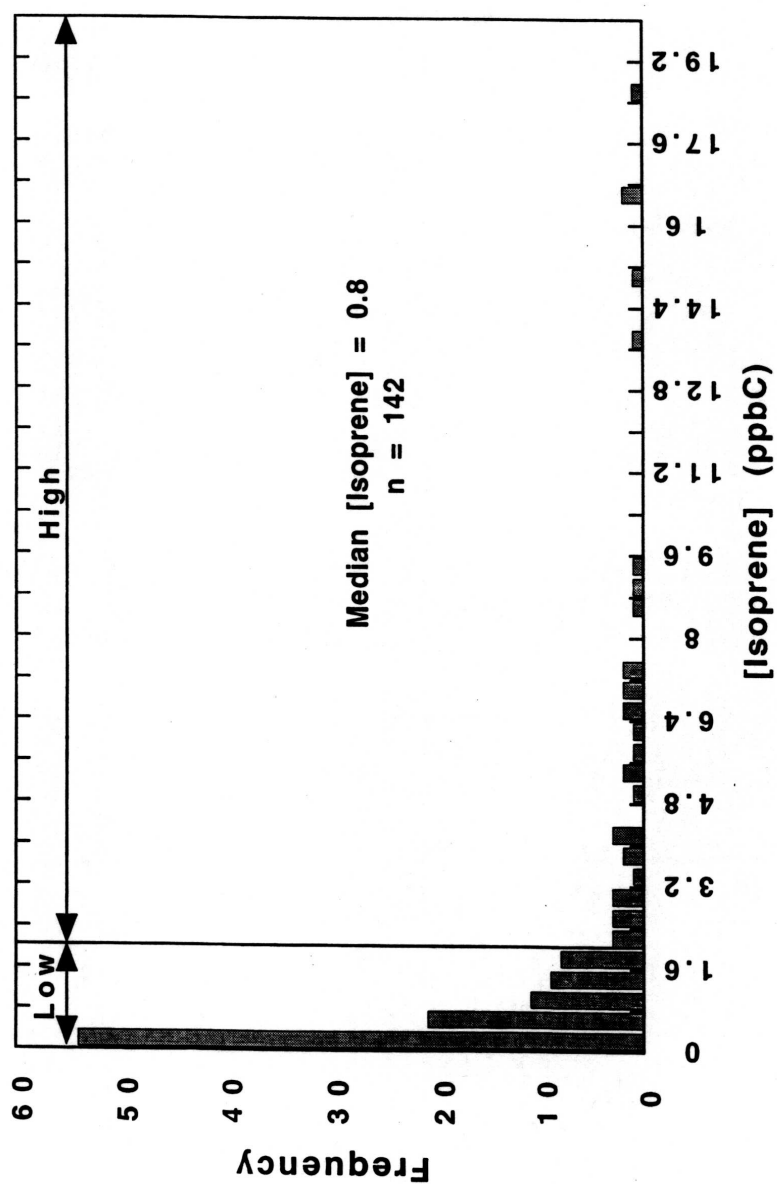


Figure 16. A study of the distribution of isoprene observations aboard the DOE-G1 over the entire SOS study. A total of 142 samples show isoprene concentrations can vary by 2 orders of magnitude. Seventy-five percent of the observations are between 0 and 2 ppb C. We have chosen to divide the data into two regimes of low isoprene concentrations (< 2 ppb C) and high isoprene concentrations (> 2 ppb C).

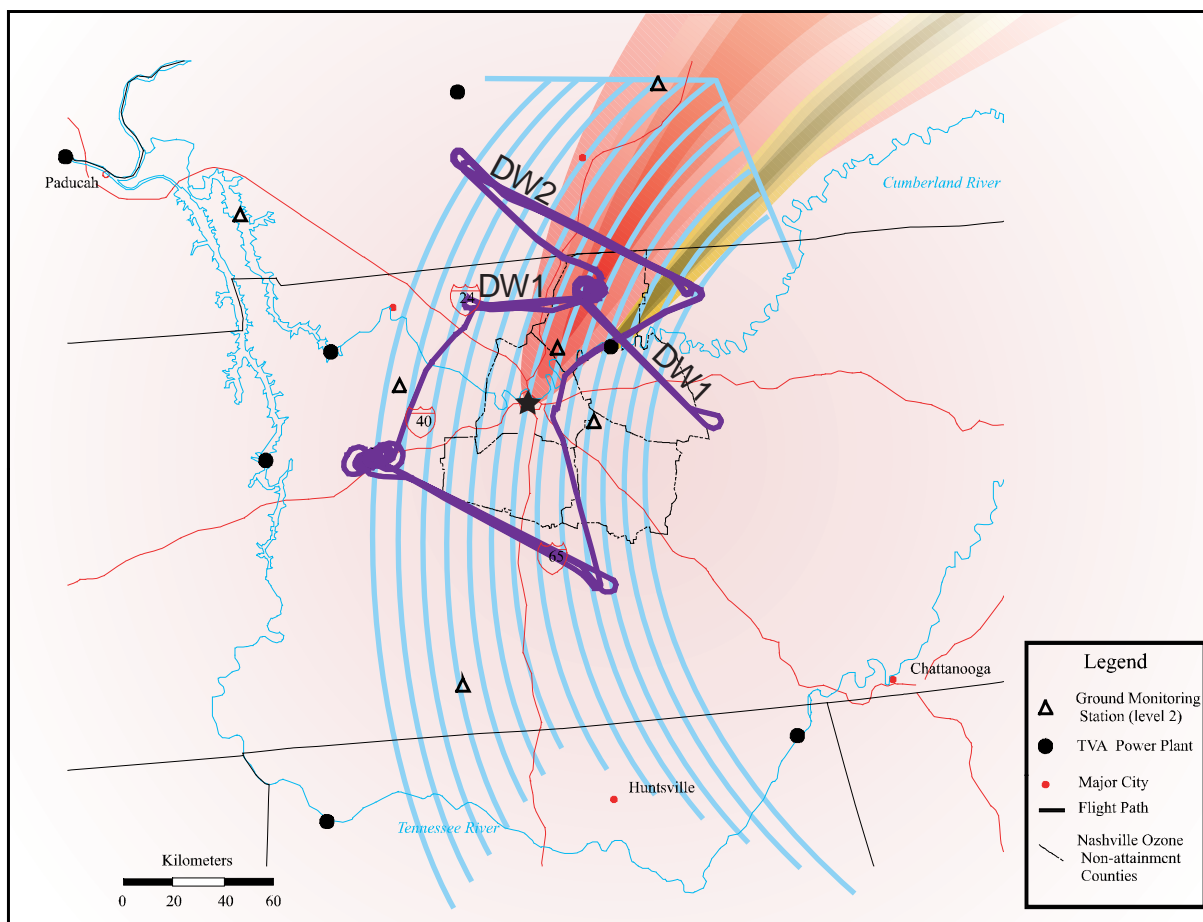


Plate 1. A map of the experimental region showing the city of Nashville at the center of the map and the flight track of the DOE G-1 on July 3, 1995. The average wind direction, established on the basis of a back trajectory is indicated by the light blue arrow. The urban and Gallatin plumes are schematically illustrated in red and yellow, respectively.

Southern Oxidants Study 3 JUL 1995

NOAA/ETL
Excimer UV-DIAL

OZONE (PPBV) from 276.9 and 291.6 nm



25 40 55 70 85 100

CASA 212, N287MA

15:14 - 19:09 UTC

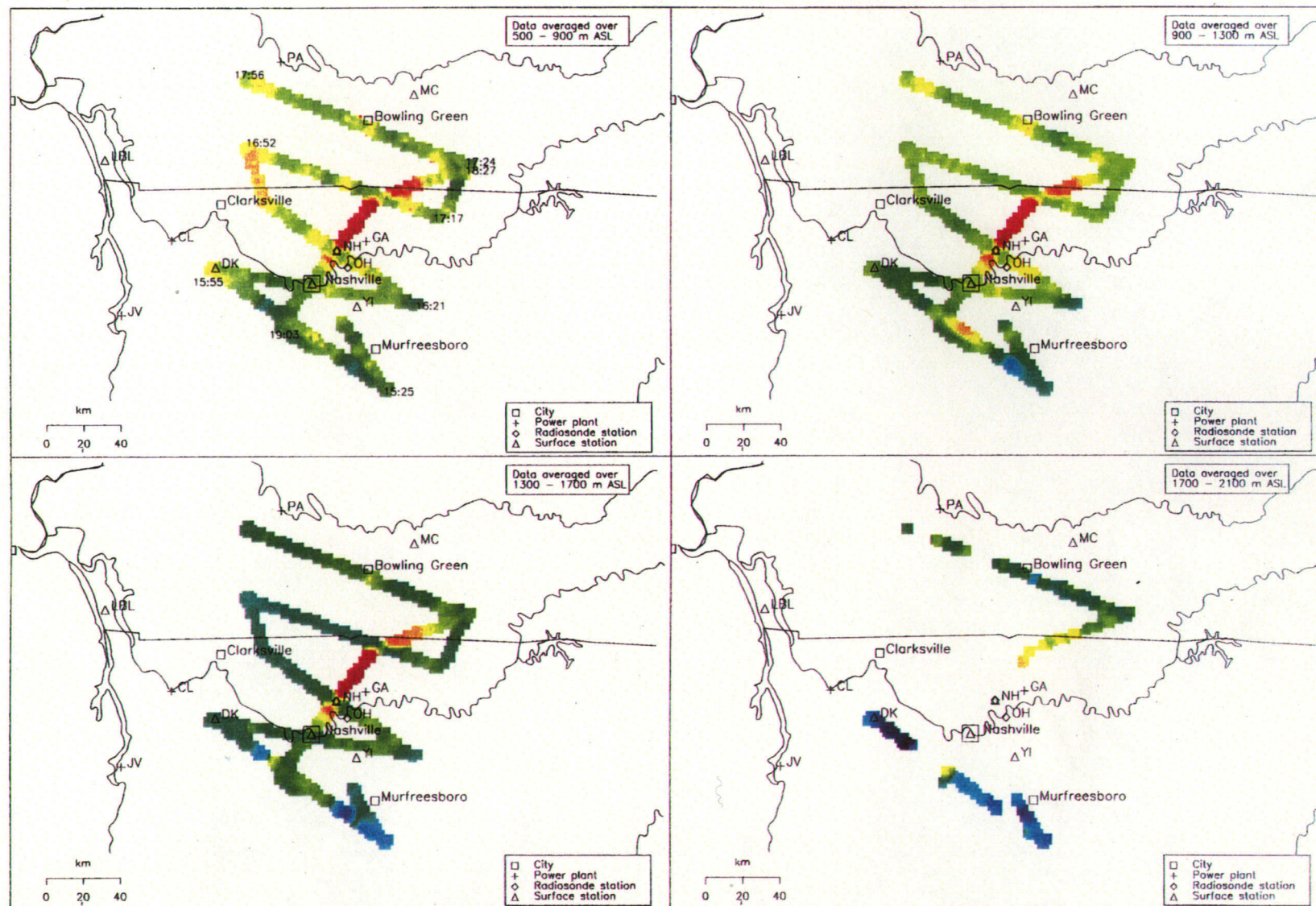


Plate 2. A false color representation of O₃ concentrations from measurements made by the NOAA-ERL CASA 212 on July 3, 1995 at various altitudes.

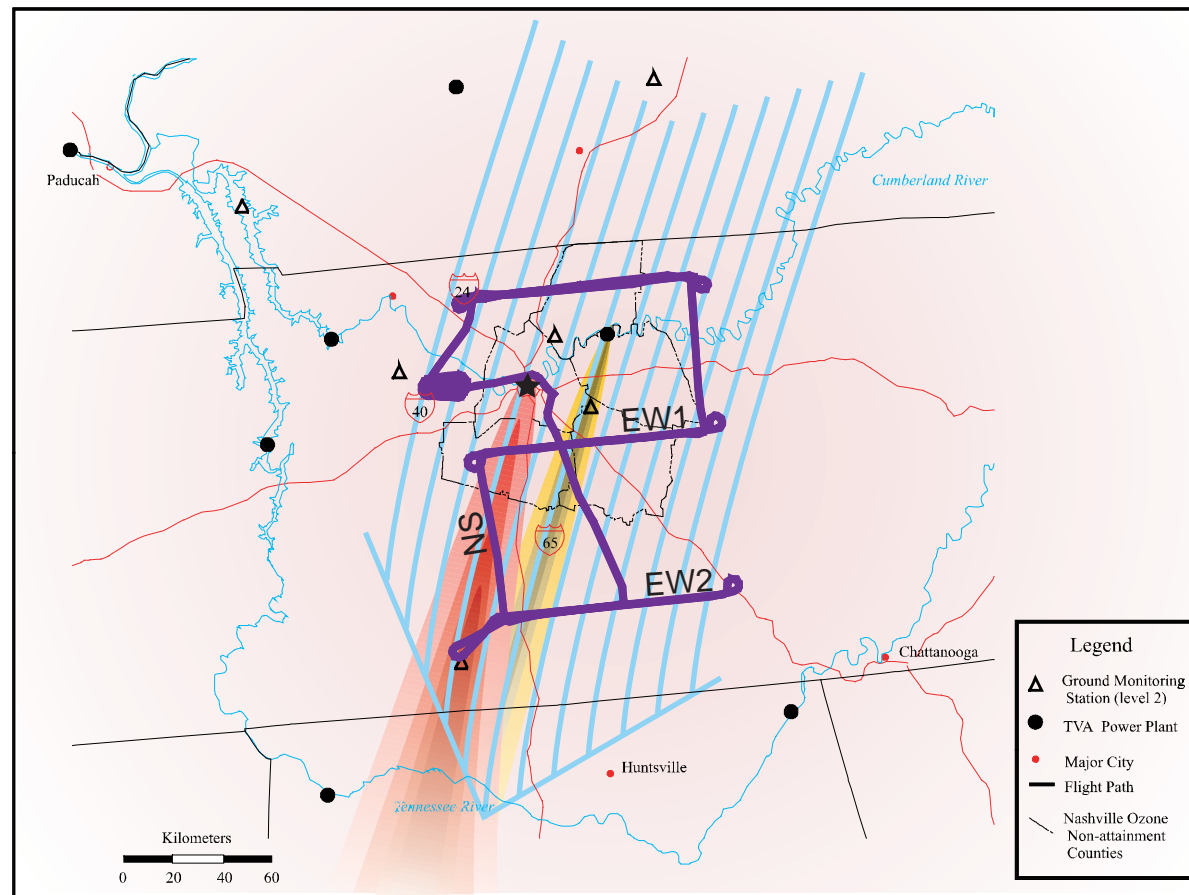


Plate 3. A map of the experimental region showing the city of Nashville at the center of the map and the flight track of the DOE G-1 on July 18, 1995. The average wind direction, established on the basis of a back trajectory, is indicated by the light blue arrow. The urban and Gallatin plumes are schematically illustrated in red and yellow, respectively.